



## Copper-incorporated magnetic nanoparticles: A reusable catalyst for Chan-Lam coupling for synthesis of N-aryl sulfonamides

Taha Najm Abdullah Aalhusaini, Gajanan S. Rashinkar\*

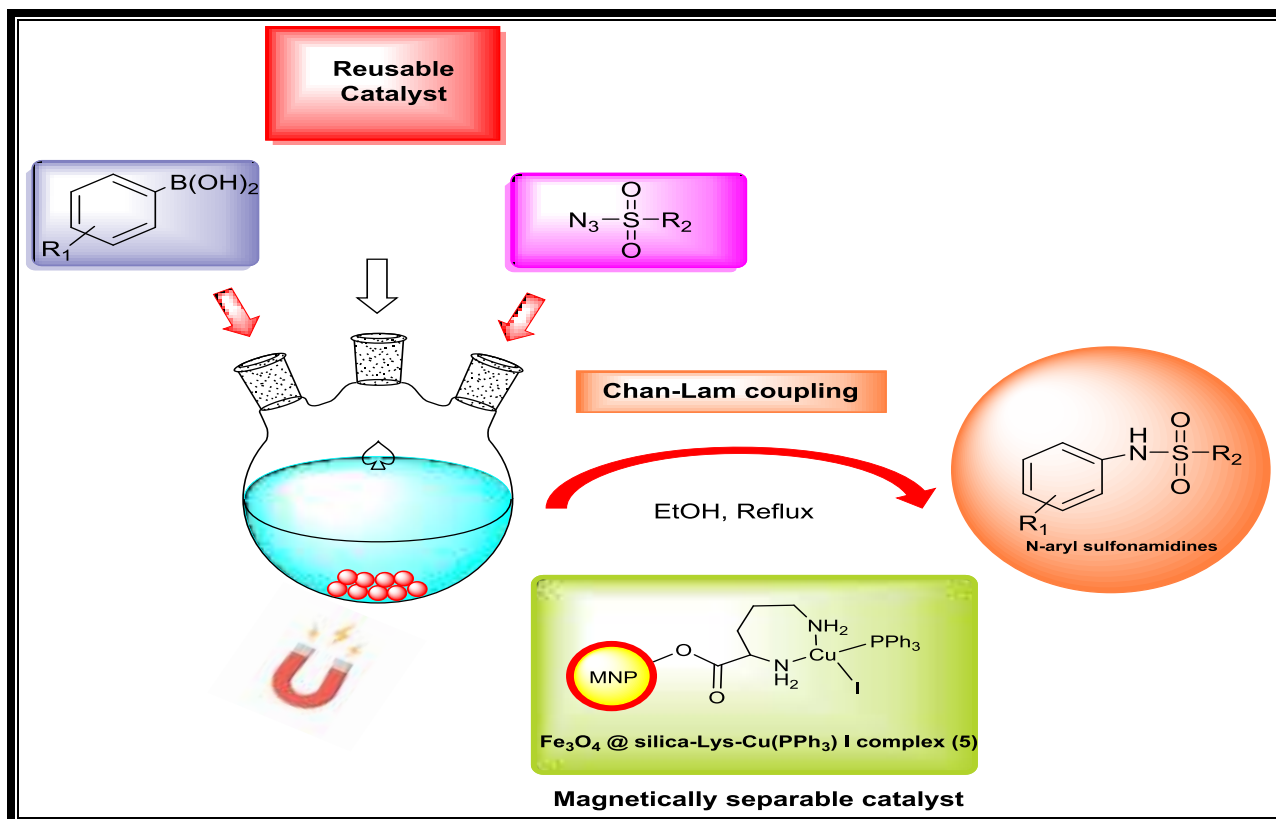
Department of Chemistry, Shivaji University, Kolhapur, 416004, M.S., India

E-mail: [tahanajem94@gmail.com](mailto:tahanajem94@gmail.com)

\*E-mail: [gsh\\_chem@unishivaji.ac.in](mailto:gsh_chem@unishivaji.ac.in)

Tel.: +91 231 260 9169; fax: +91 231 2692333

### Graphical Abstract



---

**Abstract**

This paper describes the synthesis and characterization of copper-integrated magnetic nanoparticles ( $\text{Fe}_3\text{O}_4$ @silica-Lys-Cu( $\text{PPh}_3$ )I) with a size less than 16 nm. The complex was adequately characterized by thermogravimetric analysis (TGA), Fourier transform infrared (FT-IR), energy dispersive X-ray analysis (EDX), transmission electron microscopy (TEM), X-ray photoelectron spectroscopy (XPS), X-ray diffraction (XRD), and a vibrating sample magnetometer, (VSM). Using the Chan-Lam coupling method, the catalytic performance of copper integrated magnetic nanoparticles ( $\text{Fe}_3\text{O}_4$ @silica-Lys-Cu( $\text{PPh}_3$ )I) was investigated in the preparation of bioactive N-aryl sulfonamides from a variety of aryl boronic acids and sulfonyl azides in ethanol. The key advantages of present method are magnetically separable catalyst by applying external magnet and use of green solvent. The reusability studies exhibit that complex can be reused up to eight consecutive times without material reduction in catalytic activity.

**Keywords:** Copper, green solvent, magnetic nanoparticles, N-aryl sulfonamides, reusability, triphenylphosphine.

---

**Introduction**

Recently, cross coupling reactions have emerged as an extremely useful tool in synthetic organic chemistry. By combining two fragments with the assistance of a metal catalyst, they make it possible to produce products in a straightforward manner. [1] For their potential value in medicinal chemistry, C-N cross-coupling reactions have been intensively studied, and they have made substantial contributions to the synthesis of dyes, agrochemicals, and medicines. These responses have also contributed significantly to the development of new methodologies. [2a-b] Due to the diverse applications for the products of C-N cross-coupling reactions, numerous methods have been developed. [3a-c] Chan-Lam coupling is one of the most frequently used techniques for C-N cross coupling. The Chan-Lam coupling process employs arylboronic acids in conjunction with amines under moderate reaction conditions. It has many advantages over other methods, including inexpensive catalysts, room temperature, and excellent functional group endurance. Moreover, the Chan-Lam coupling reaction can be performed in a single step. [4a-c] Their synthesis of antidepressant drugs, N-arylation of purine nucleosides, derivatization of silica gel exterior, creation of a porous aromatic structure, fabrication of a microelectrode array with a polymer coating for electrochemical signalling, etc. all utilise the Chan-Lam coupling. [5] In recent years, the development of magnetic nanoparticles (MNPs) has been accelerated in the catalysis industry, where magnetic nanocatalysts are essential for meeting green chemistry requirements. [6a-m]. Using MNPs is one way to link homogeneous and heterogeneous catalysis in a chemical reaction. [6n] MNPs are utilised for a variety of applications, including catalysis[7], biomedical engineering[8a-d], therapeutic delivery[8e], biosensor[8f], atmospheric treatment[9], biochemical separation[10], biocompatibility [11] and dietary analysis[12]. Since the surfaces of MNPs can be functionalized with such a wide variety of substrates, this has created a multitude of opportunities for designing mission catalysts. [13a]

Organosiloxane precursors have been utilised successfully for depositing silica on MNPs, among numerous other precursors. This coating functions as a barrier and hydroxyl-rich layer for a significant amount of organofunctionalization. Other materials have been utilised as well. [13b] MNPs have recently gained traction as potentially useful advanced materials due to their unique combination of physicochemical properties, which include strong dispersivity, massive surface area, low harmful potential, super-paramagnetic performance, and bioactivity. [13c] As a result, nano-magnetite-assisted catalytic systems have recently generated a great deal of interest within the field of chemical synthesis. [14] In addition, the prospect of magnetically separated catalysis has attracted the interest of the academic community, not least because of its potential application in fixed-bed systems and the ease with which it can be retrieved using an external magnet. [15] Despite progress, MNP development in magnetic findable catalyst preparation is still in its infancy and requires immediate attention. N-aryl sulfonamides are preferred patterns that have been demonstrated to play an active role in the study of biological sciences due to their fascinating chemical properties and potential biological actions. In contrast to their use in treating diabetes, hydrops, and cardiovascular issues, these compounds exhibit analgesic, carcinogenic, antiseptic, and acquired immune deficiency syndrome properties. [16] The production of N-aryl sulfonamides is a major focus of research in the field of chemical synthesis due to the compounds' promising medical applications. Copper catalysed interactions of sulfonyl azides or sulfonamides with boronic acids,[17] and palladium(II) acetate catalysed N-arylation of sulfonamides involving haloarenes or aryl triflates,[18] to name a few of the most well-known techniques. Transition metal-free reaction of o-silylaryl triflates with sulfamides;[19] copper facilitated the reaction of chloramine-T and arylboronic acids;[20a] Pd aided the cross-coupling of methanesulfonamide with haloarenes; [19b] Pd enhanced the aminosulfonylation of aryl iodides; and [20c] iron catalyzed the [20d] In terms of substrate versatility, moderate reaction conditions, and potential synthetic applications, the copper-catalyzed reaction of sulfonyl azides and boronic acids is the most efficient method. Recent research indicates that a variety of catalytic systems may increase the effectiveness of this method. In addition, there is still room for investigation of novel methods, particularly those involving the use of a substantial catalyst support. Using ethanol and the Chan-Lam coupling method, we present a novel method for producing bioactive N-aryl sulfonamides from a variety of aryl boronic acids and sulfonyl azides. This method is a continuation of our work on heterogeneous catalysis and is based on the discussion presented above. [21]

## **2. Experimental section**

### **2.1 General remarks**

The reactions were conducted with dried equipment, which also served to maintain the necessary conditions for the reactions. To verify the product and surface functionalization, KBr pellets were utilized in a Perkin-Elmer Spectrometer (Model No.783USA) to obtain FTIR spectra of compounds in the range of 400–4000  $\text{cm}^{-1}$ . The weight reduction graphs were acquired by heating the sample from 25 to 1000  $^{\circ}\text{C}$  using the TA SDT Q600 V20.9 Build 20 instrument.

The elemental composition was broken down and examined using a Perkin-Elmer 2400, Series II, CHNS/O analyzer. The RIGAKU Mini flex 600 XRD was utilized for phase identification and structural elucidation of the synthesized compounds over a 2 $\theta$  angle range of 20 to 80 degrees. The morphology of the samples was examined using a Philips CM 200 electron microscope with a working voltage ranging from 20 to 200 kV. Using a Lakeshore magnetometer from the United States, Model 7410 and investigations into magnetism were conducted (VSM). All samples were induction heated in a 1.5 mL plastic microcentrifuge tube with a 6 cm diameter coil (4 turns). Following the procedure outlined in previous research, Fe<sub>3</sub>O<sub>4</sub> MNPs (**1**) and silica-coated Fe<sub>3</sub>O<sub>4</sub> MNPs (**1**) were produced (**2**). The remaining chemicals were purchased from regional suppliers and utilized without additional purification.

## 2.2 Preparation of Fe<sub>3</sub>O<sub>4</sub> MNPs(**1**)

Using chemical co-precipitation, Fe<sub>3</sub>O<sub>4</sub> nanoparticles were manufactured. In a procedure that exemplifies the method, 2 g (10 mmol) of FeCl<sub>2</sub>.4H<sub>2</sub>O and 4 g (15 mmol) of FeCl<sub>3</sub>.6H<sub>2</sub>O were dissolved in 30 ml of distilled water. In addition, 25 mL of ammonium hydroxide solution was added while vigorously agitating the aforementioned mixture. Each drop of the solution was added while the mixture was continuously stirred. After the reaction was complete, the resulting mixture sat for an additional half-hour to form the black Fe<sub>3</sub>O<sub>4</sub> MNPs precipitate. To purify the Fe<sub>3</sub>O<sub>4</sub> MNPs (**1**), we first separated them with an external magnet, then washed them with hot water, and finally dried them at 60 °C in a vacuum.

FT-IR (KBr, thin film): =3405, 1599, 570 cm<sup>-1</sup>.

## 2.3 Preparation of silica coated Fe<sub>3</sub>O<sub>4</sub> MNPs(**2**)

Nanoparticles of Fe<sub>3</sub>O<sub>4</sub> were manufactured *via* chemical co-precipitation. 2 g (10 mmol) of FeCl<sub>2</sub>.4H<sub>2</sub>O and 4 g (15 mmol) of FeCl<sub>3</sub>.6H<sub>2</sub>O were dissolved in 30 mL of distilled water as an example of the method. In addition, 25 mL of ammonium hydroxide solution was added to the mixture while vigorously stirring. Each drop of the solution was added while continuously stirring the mixture. After the reaction was complete, the mixture was sat for an additional half-hour to precipitate the black Fe<sub>3</sub>O<sub>4</sub> MNPs. The Fe<sub>3</sub>O<sub>4</sub> MNPs (**1**) were purified by separating them with an external magnet, washing them with hot water, and then drying them at 60 °C in a vacuum. FT-IR (KBr, thin film): = 3410, 1602, 1072, 971, 795 and 634 cm<sup>-1</sup>.

## 2.4 Preparation of Fe<sub>3</sub>O<sub>4</sub>@silica-Lys (**4**)

The mixture of silica coated Fe<sub>3</sub>O<sub>4</sub> MNPs (**2**) (2 g) and L-Lysine (**3**) (2 g, 13 mmol) dissolved in distilled water (100 mmol) was continuously stirred for an hour and a half. After allowing the reaction mixture to settle completely, magnetic separation was utilized to separate the product. Fe<sub>3</sub>O<sub>4</sub>@silica-Lys (**4**) was obtained by treating the product with methanol (4 x 20 mL), distilled water (4 x 20 mL), and drying it under vacuum at 50 °C for 13 hours (**4**).

FT-IR (KBr, thin film): = 3404, 2924, 1741, 1384, 1101, 971, 813 and 638 cm<sup>-1</sup>.

## 2.5 Preparation of [Fe<sub>3</sub>O<sub>4</sub>@silica-Lys-Cu(PPh<sub>3</sub>)I]complex (**5**)

A mixture of MNP-Lys (**4**) (2.0 g), CuI (0.95 g, 5 mmol) and triphenyl phosphine (1.3 g, 5 mmol) in distilled water (100 mL) was stirred at 80 °C for 24 h. Afterwards, the product was

separated by external magnet, washed with methanol ( $3 \times 50$  mL),  $\text{CH}_2\text{Cl}_2$  ( $3 \times 50$  mL) and dried under vacuum at  $50^\circ\text{C}$  for 24 h to yield  $[\text{Fe}_3\text{O}_4@\text{silica-Lys-Cu}(\text{PPh}_3)\text{I}]$  complex (**5**).

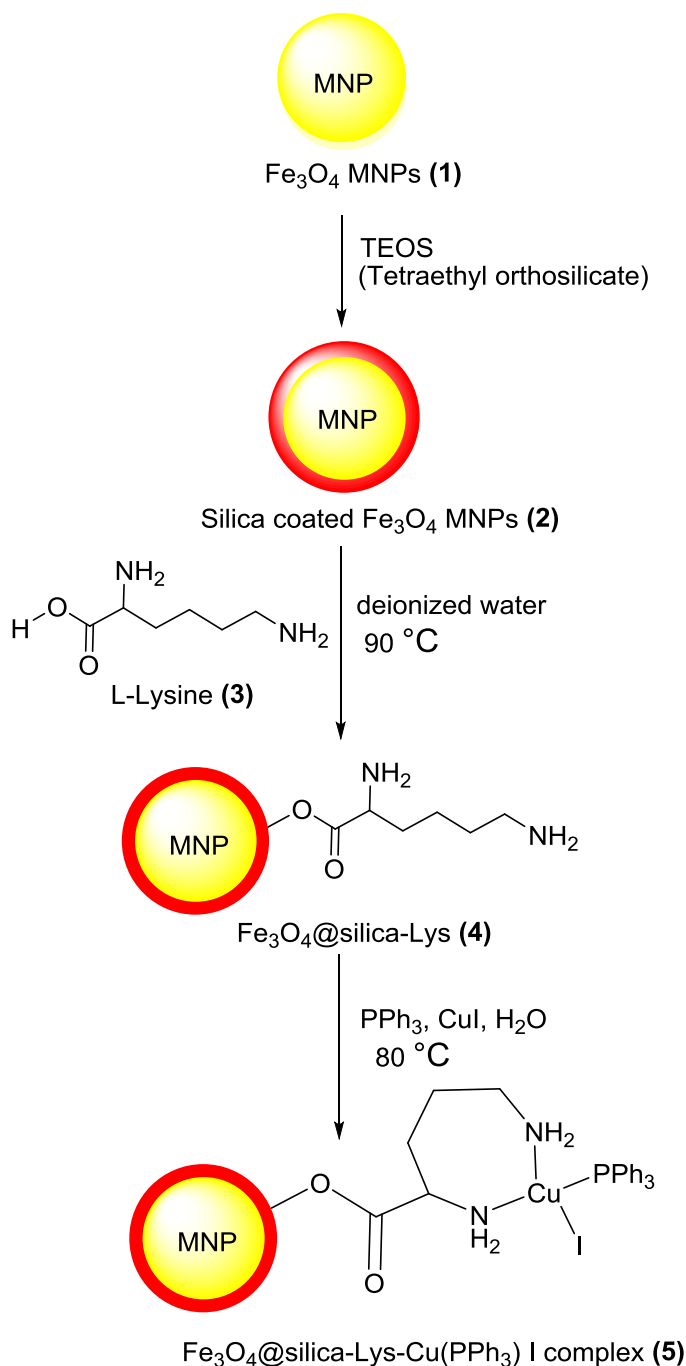
FT-IR (KBr, thin film):  $\nu = 3418, 2958, 2923, 1675, 1634, 1564, 1518, 1480, 1434, 1094, 693, 515, 469\text{ cm}^{-1}$ . Observed analysis of elements (%): C, 33.80; N, 0.84; P, 3.19; O, 22.82; Si, 11.67; Fe, 18.46; Cu, 4.37; I, 1.80; Loading:  $0.68\text{ mmol Cu g}^{-1}$  of **5**.

### **2.6 Protocol for the general synthesis of N-aryl sulfonamides**

A mixture of phenyl boronic acid (1.2 mmol), sulfonyl azide (1 mmol) and  $[\text{Fe}_3\text{O}_4@\text{silica-Lys-Cu}(\text{PPh}_3)\text{I}]$  complex (**5**) (70 mg) in ethanol (5 mL) was stirred at  $70^\circ\text{C}$ . After completion of the reaction as monitored by the TLC, the **5** was Separated by using external magnet. Evaporation of solvent in vacuum followed by column chromatography over silica gel using petroleum ether-ethyl acetate afforded pure products.

### **3. Results and discussion**

Preparation of Magnetic nanoparticle decorated Lysine-copper complex is depicted in scheme 1. Initially, water dispersible base  $\text{Fe}_3\text{O}_4$  MNPs (**1**) were prepared by chemical precipitation method as described in the literature.[22] The silica coating of **1** was achieved through base catalyzed hydrolysis using tetraethyl orthosilicate (TEOS) resulting in the formation of silica coated  $\text{Fe}_3\text{O}_4$  MNPs (**2**).[23] The organofunctionalization of **2** with L-lysine (**3**) resulted in the formation  $\text{Fe}_3\text{O}_4@\text{silica-Lys}$  (**4**) through the reaction of  $-\text{COOH}$  groups of **3** with  $-\text{Si-OH}$  groups of **2** forming stable O-Si-O bonds. We have chosen L-lysine as a prime ligand owing to the presence of groups that serve as donor ligands forming stable chelates with variety of metals ions. Finally, the complexation of **4** with  $\text{Ph}_3\text{P}$  as a co-ligand and  $\text{CuI}$  as metal salt precursors resulted in the formation of desired copper incorporated magneticnanoparticles acronymed as  $\text{Fe}_3\text{O}_4@\text{silica-Lys-Cu}(\text{PPh}_3)\text{I}$  complex (**5**).



**Scheme 1:** [Fe<sub>3</sub>O<sub>4</sub> @ silica-Lys-Cu(PPh<sub>3</sub>)I] synthesis in multiple steps complex (5)

**3.1 FT-IR:-** The FTIR spectroscopy was used to monitor the reaction sequence employed for the synthesis of [Fe<sub>3</sub>O<sub>4</sub>@silica-Lys-Cu(PPh<sub>3</sub>)I] complex (5). The FTIR spectrum of Fe<sub>3</sub>O<sub>4</sub> MNPs (1) displayed characteristic Fe–O stretching band at 570 cm<sup>-1</sup> (Figure 1[a]). The FTIR bands at 1101 cm<sup>-1</sup>, 971 cm<sup>-1</sup>, and 813 cm<sup>-1</sup> corresponding to a symmetric Si–O–Si stretching, symmetric Si–O–Si stretching, and asymmetric Si–O–Si stretching, respectively suggests the formation of

silica coated  $\text{Fe}_3\text{O}_4$  MNPs (**2**)(**Figure 1[b]**)[24]. The successful covalent grafting of L-lysine (**3**) on **2** was corroborated from the FTIR spectra of  $\text{Fe}_3\text{O}_4$ @silica-Lys (**4**) that displayed peaks at 3404 (N-H stretching), 2924 (C-H stretching), 1635 (C=O stretching), 1462 (C-O stretching), 1384 (C-N stretching) and  $638\text{ cm}^{-1}$  (Fe-O stretching) (**Figure 1[c]**)[25,26]. Finally, the formation of **5** was validated from the FTIR spectrum which revealed characteristic peaks at  $693\text{ cm}^{-1}$  (Cu-I stretching) and series of bands in the region  $1094\text{-}515\text{ cm}^{-1}$  corresponding to the stretching of P-C bonds in  $\text{PPh}_3$  group.[27,28] Further, the formation of **5** was supported from appearance of strong peaks at  $1634\text{ cm}^{-1}$  (symmetric C-C stretching),  $1480\text{ cm}^{-1}$ , and  $1434\text{ cm}^{-1}$  (stretching vibrations of the monosubstituted benzene ring) (**Figure 1[d]**).[29]

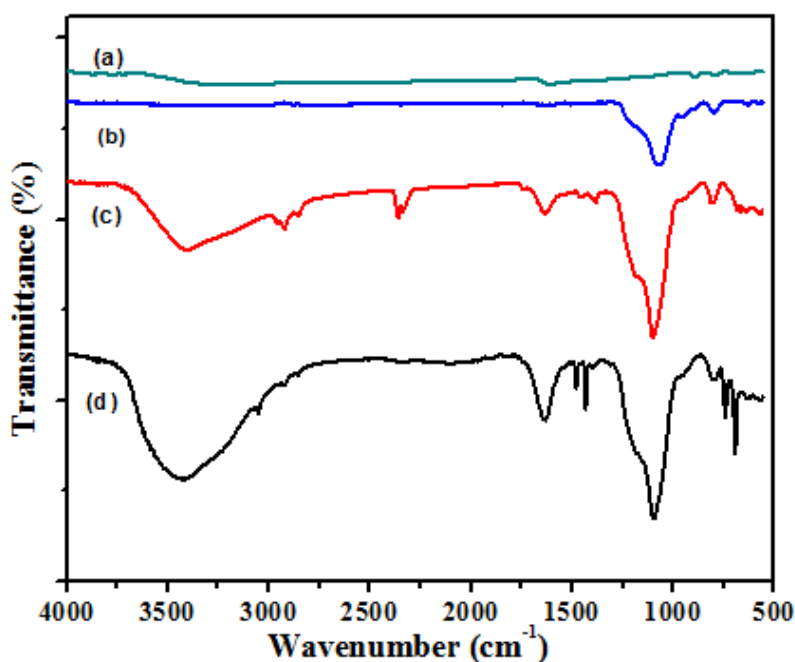


**Figure 1:** FT-IR spectra of [a]  $\text{Fe}_3\text{O}_4$  MNPs (**1**); [b] Silica coated  $\text{Fe}_3\text{O}_4$  MNPs (**2**); [c]  $\text{Fe}_3\text{O}_4$ @silica-Lys(**4**); [d] [ $\text{Fe}_3\text{O}_4$ @silica-Lys-Cu( $\text{PPh}_3$ )I] complex (**5**)

**3.2 TGA:-** The thermal profile of base  $\text{Fe}_3\text{O}_4$  MNPs (**1**) and [ $\text{Fe}_3\text{O}_4$ @silica-Lys-Cu( $\text{PPh}_3$ )I] complex (**5**) was investigated by using thermogravimetric analysis(TGA) over the temperature range of  $25\text{-}1000\text{ }^\circ\text{C}$  at a heating rate of  $10\text{ }^\circ\text{C}/\text{min}$  under nitrogen environment (**Figure 2**). The TGA curve of **1** depicted two stage thermal decomposition (**Figure 2[a]**). The first weight loss of 5.27% up to  $129\text{ }^\circ\text{C}$  is attributed to the evaporation of water. The existence of  $\text{Fe}_3\text{O}_4$  molecules was confirmed by a lack of noticeable second weight loss between  $130\text{-}800\text{ }^\circ\text{C}$ . (**Figure 2[a]**). On the contrary, thermogram of **5** revealed multi-stage thermal decomposition pattern. An initially, weight loss of 3.96% up to  $160\text{ }^\circ\text{C}$  was ascribed to desorption of physisorbed and chemisorbed water. The cumulative three-step weight loss of 6.82%, 25.79%, and 13.80% is attributed to the decomposition of organic moieties functionalized on the  $\text{Fe}_3\text{O}_4$  core. Finally, the large residue

weight of 45.92% is due to formation of metallic oxide and carbaceneous material.[30.31](Figure 2[b]).

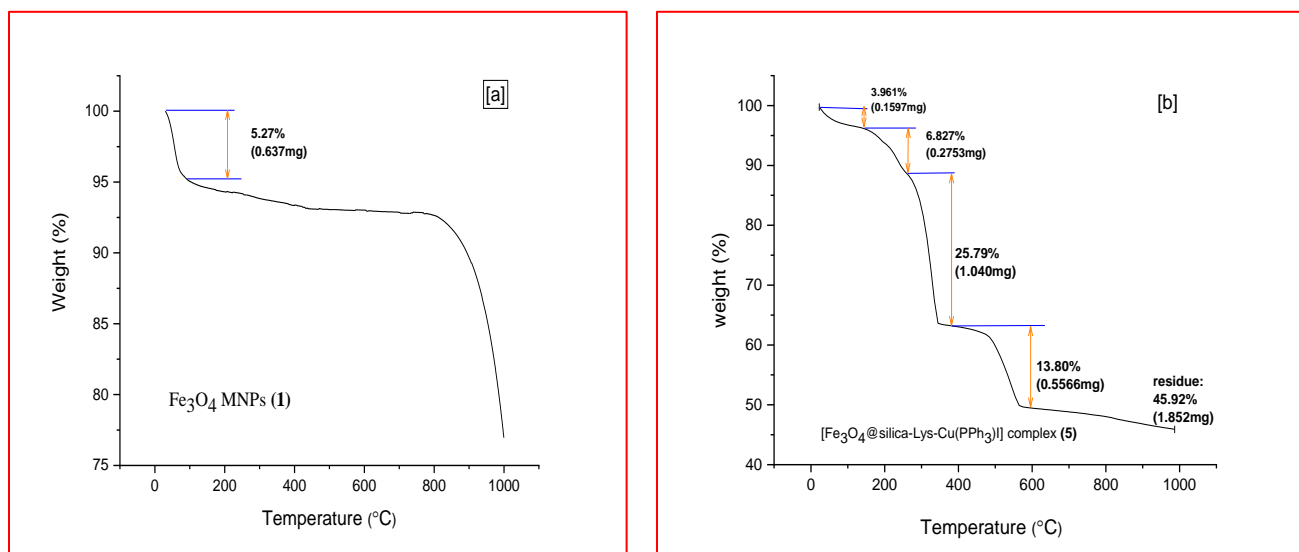


**Figure 2:** TGA curves of [a]Fe<sub>3</sub>O<sub>4</sub> MNPs (**1**) and [b][Fe<sub>3</sub>O<sub>4</sub>@silica-Lys-Cu(PPh<sub>3</sub>)I] complex (**5**)

**3.3 EDX:** -Energy dispersive x-ray analysis (EDX) was utilized to analyze the elements composition of [Fe<sub>3</sub>O<sub>4</sub>@silica-Lys-Cu(PPh<sub>3</sub>)I] complex (**5**). The EDX mapping revealed the presence of carbon, oxygen, iron, nitrogen, phosphorus, silicon, and copper (**Figure 3**). The analysis revealed 4.34% of Cu indicating loading of 0.68 mmol of Cu per gram of **5**.

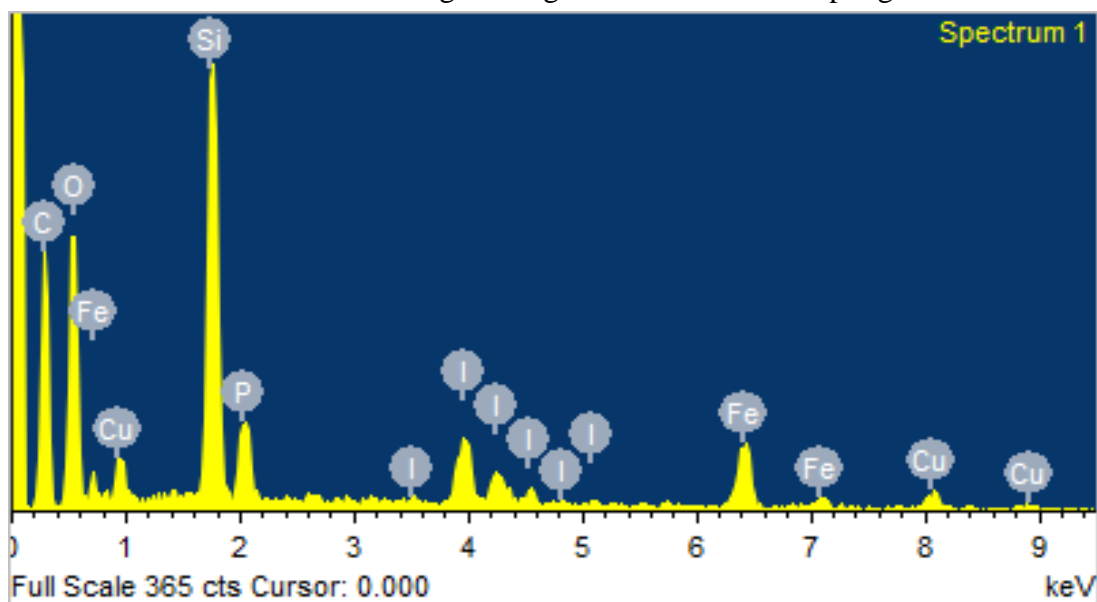


**Figure 3:** EDX spectra of [Fe<sub>3</sub>O<sub>4</sub>@silica-Lys-Cu(PPh<sub>3</sub>)I] complex (**5**)

**3.4 XRD:** - (XRD) examination was utilized to determine if the crystal structure of  $\text{Fe}_3\text{O}_4$  MNPs (**1**) was maintained in  $[\text{Fe}_3\text{O}_4@\text{silica-Lys-Cu}(\text{PPh}_3)\text{I}]$  complex **5**. (**Figure 4**). With (hkl) values of (220), (311), (400), (331), and (431), the major distinctive peaks in the diffractogram of **5** were formed well with (220), (311), (400), (331), (431) and (511).[32] All of the reflective peaks were referenced on the JCPDS card (reference code: 77-1545), indicating that the  $\text{Fe}_3\text{O}_4$  MNPs have a single phase inverse spinel structure with high phase crystallization. Using the Debye-Scherrer formula, the average crystal size was calculated to be 15.9 nm based on the most prominent peaks (311) at  $2\theta$  values of  $35.54^\circ$  for **5**. The accuracy of this calculation's results was confirmed. XRD analysis reveals that the crystalline structure of compound **1** is maintained even after undergoing multi-step functionalization in compound **5**.

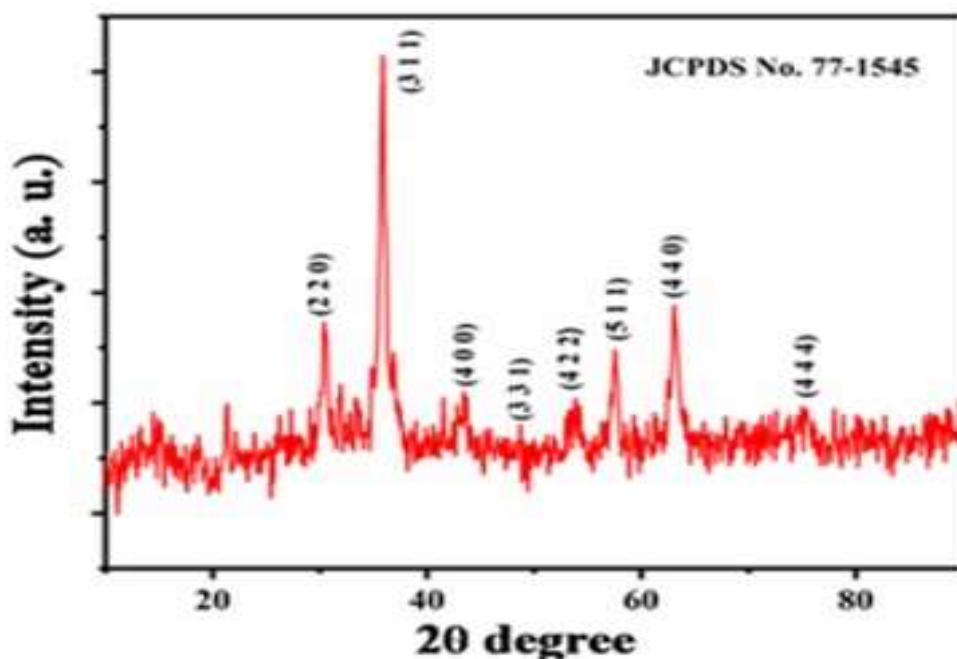


**Figure 4** XRD pattern of  $[\text{Fe}_3\text{O}_4@\text{silica-Lys-Cu}(\text{PPh}_3)\text{I}]$  complex (**5**)

**3.5 TEM:** - Transmission electron microscopy (TEM) was used to investigate the morphology of the  $[\text{Fe}_3\text{O}_4@\text{silica-Lys-Cu}(\text{PPh}_3)\text{I}]$  complex (**5**). The TEM micrographs(**Figure 5**)revealed spheres with non-smooth surface. Moreover, encapsulated dark magnetite nanocores surrounded by grey shell were seen in TEM micrographs(**Figure 5a-b**).[33] A fine observation of (**Figure 5c**)indicate average nanoparticle size of 15 nm for **5** with a lattice fringe width distance of  $d_{(311)} = 2.516 \text{ \AA}$ . Selected Area Electron diffraction (SAED) of **5** exhibit four strong diffraction rings with bright dotted pattern corresponding to crystallographic planes (311), (400), (331) and (422) respectively (**Figure 5d**). SAED pattern of **5** persuades polycrystalline nature of  $\text{Fe}_3\text{O}_4$  MNPs.

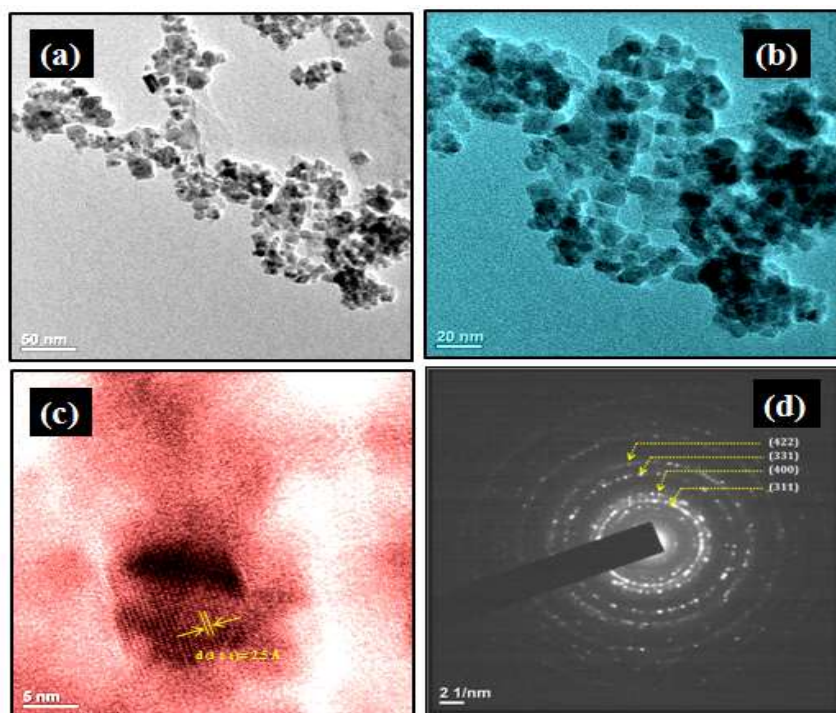


**Figure 5:** TEM images of [a-b] [Fe<sub>3</sub>O<sub>4</sub>@silica-Lys-Cu(PPh<sub>3</sub>)I](5);

[c] Nanoparticle of **5** showing lattice fringe width; [d] SAED pattern of **5**

**3.6 VSM:** -The magnetic properties of Fe<sub>3</sub>O<sub>4</sub> and [Fe<sub>3</sub>O<sub>4</sub>@silica-Lys-Cu(PPh<sub>3</sub>)I]**5** were evaluated by vibrating sample magnetometer (VSM) measurements. The VSM analysis revealed saturation magnetism (M<sub>s</sub>) value of 75 emu g<sup>-1</sup> for **1** and 52 emu g<sup>-1</sup> for **5** (Fig. 6a-b). The decrease in the M<sub>s</sub> value caused by the presence of organofunctional groups on the nano-exterior magnetite's.[34] Even though M<sub>s</sub> values of **5** is lower than that of **1**, it is sufficient to allow facile separation using an external magnet.

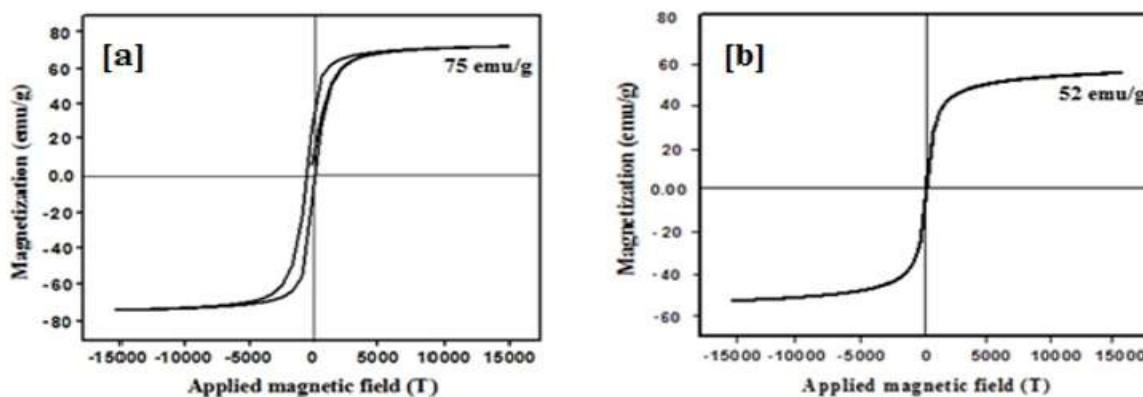


**Figure 6** Magnetic curves of [a]bare Fe<sub>3</sub>O<sub>4</sub> MNPs (**1**)and [b] [Fe<sub>3</sub>O<sub>4</sub>@silica-Lys-Cu(PPh<sub>3</sub>)I] complex (**5**)

**3.7 XPS:** -The X-ray photoelectron spectroscopy (XPS) was further employed for structural investigations of  $[\text{Fe}_3\text{O}_4@\text{silica-Lys-Cu}(\text{PPh}_3)\text{I}]$  complex (**5**). The XPS survey spectrum of  $[\text{Fe}_3\text{O}_4@\text{silica-Lys-Cu}(\text{PPh}_3)\text{I}]$  complex (**5**) displayed peaks of Fe, O, Si, C, N, P, I and Cu (**Fig. 7a**). The core level XPS spectrum of Cu 2p displayed peaks at 933.44 eV and 953.45 eV respectively (**Fig. 7b**). The fact that the energies of these peaks differ by 20.01 eV demonstrates that copper in complex **5** is in +1 oxidation state.[35] In the core level XPS spectrum of C1s, the main peak is observed at 285.1 eV which is again deconvoluted into 283.1 eV (**Fig. 7c**). The peak at 283.1 eV shows bonding interactions of carbon and silicon. This fact is again confirmed by a peak around 100.6 eV in the Si 2p region (**Fig. 7a**). The core level spectrum of oxygen displays peaks with binding energies 529.7 and 533.2 eV which are indicative for oxygen in  $\text{Fe}_3\text{O}_4$  and oxygen bonded with Si (**Fig. 7d**).[36] The large peak area with binding energy 131.77 eV is ascribed to presence of P 2p peak related to triphenylphosphine group (**Fig. 7e**). A pronounced peak displayed with binding energy 401 eV confirms N atom bonded in  $\text{NH}_2$  group (**Fig. 7e**). These observations strongly suggest the coordination of  $\text{NH}_2$  with Cu (**Fig. 7f**). In addition, the peak at 631 eV results from iodine interacting with the covalently bonded copper atom in copper iodide. At 712 and 728 eV, the core level XPS spectrum of the element Fe 2p displays a pair of solitary peaks. The findings of this study provide conclusive evidence for the successful formation of **5** and confirm the proposed structure.

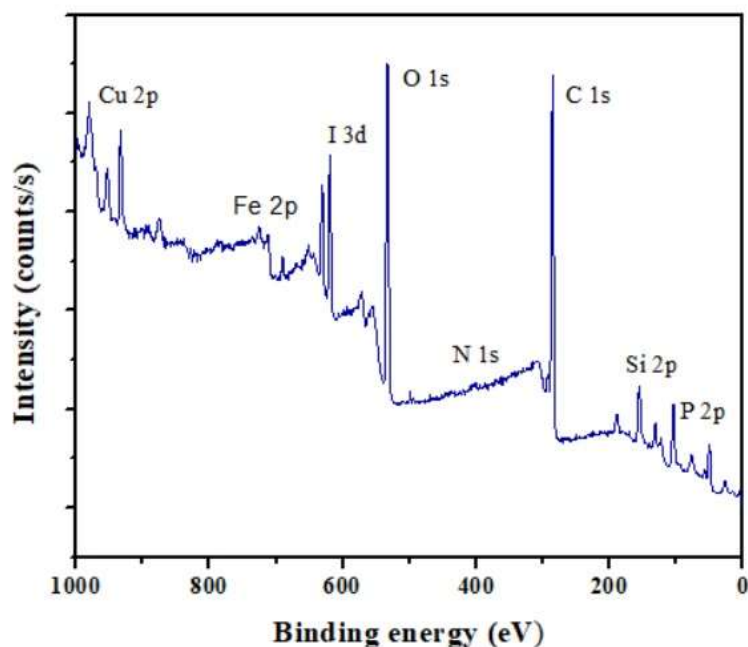
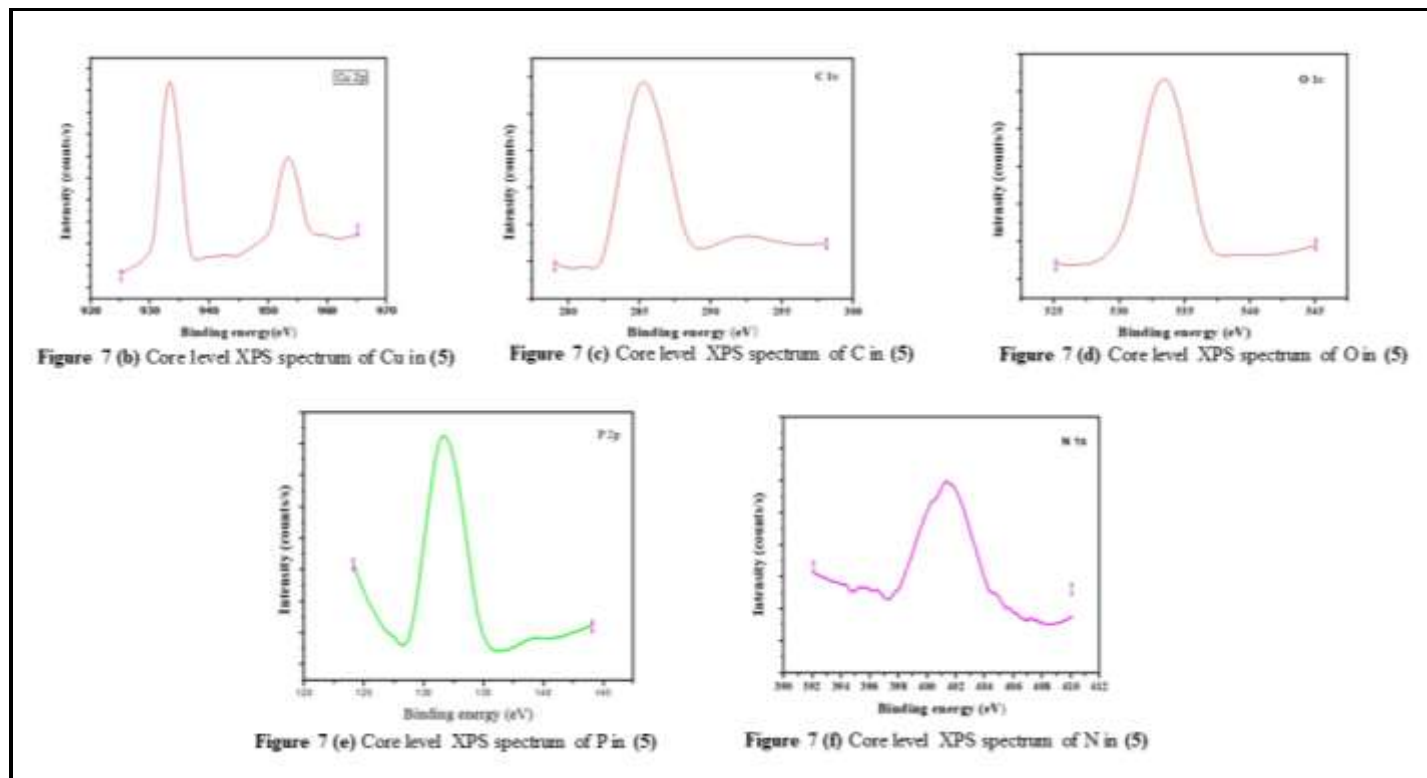
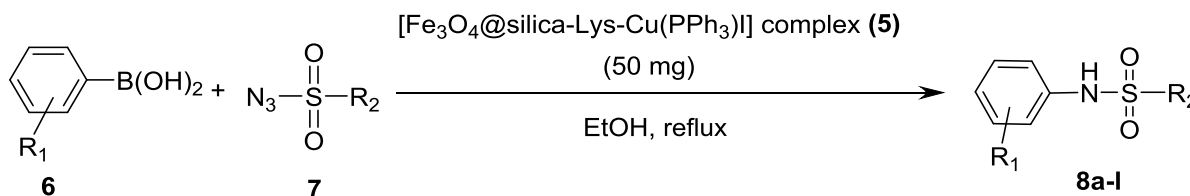


**Figure 7 (a)** XPS survey spectrum of  $[\text{Fe}_3\text{O}_4@\text{silica-Lys-Cu}(\text{PPh}_3)\text{I}]$ . complex (**5**)



During the subsequent step, the synthesis of N-aryl sulfonamides, the catalytic performance of the  $[\text{Fe}_3\text{O}_4@\text{silica-Lys-Cu}(\text{PPh}_3)\text{I}]$  complex (**5**) was investigated (**Scheme 2**).



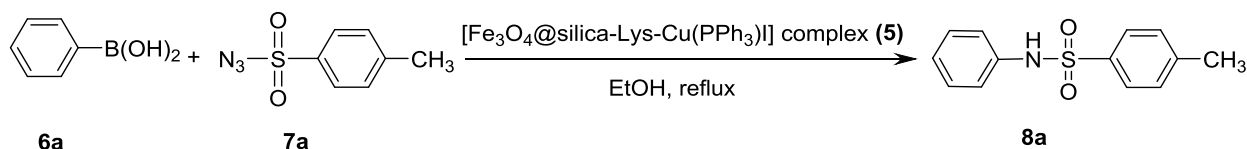
**Scheme2-**  $[\text{Fe}_3\text{O}_4@\text{silica-Lys-Cu}(\text{PPh}_3)\text{I}]$  complex (**5**) was responsible for the catalysis of the formation of N-aryl sulfonamides.

To determine the optimal conditions for the synthesis, we exhaustively screened multiple variables. We used phenyl boronic acid (**6a**; 1.2 mmol) and 4-toluenesulfonyl azide as typical substrates (**7a**; 1.0 mmol). Numerous amounts of bare  $\text{Fe}_3\text{O}_4$  MNPs (**1**), silica layered  $\text{Fe}_3\text{O}_4$  MNPs (**2**), and  $\text{Fe}_3\text{O}_4@\text{silica-Lys}$ (**4**) were utilized in the model reaction to investigate the active site in the  $[\text{Fe}_3\text{O}_4@\text{silica-Lys-Cu}(\text{PPh}_3)\text{I}]$  complex (**5**) that is responsible for the catalytic cycle (**Table 1, entry 1-3**). Curiosity-inducingly, none of the catalytic runs resulted in the anticipated progression of the reaction. On the basis of these findings, we have determined that  $[\text{Fe}_3\text{O}_4@\text{silica-Lys-Cu}(\text{PPh}_3)\text{I}]$  complex (**5**) was the only catalyst that drove the reaction in the desired direction.

Initial research employed various concentrations of  $[\text{Fe}_3\text{O}_4@\text{silica-Lys-Cu}(\text{PPh}_3)\text{I}]$  complex (**5**) will investigate the effect of catalyst loading on the formation of N-aryl

sulfonamides. In a brief (30 minute) reaction involving 50 mg (0.034 mmol) of **5**, a high yield (94%) of 4-methyl-*N*-phenylbenzenesulfonamide (**8a**) was produced (**Table 1, entry 4**). When the process quantity was increased from 100 mg (0.068 mmol) to 150 mg (0.102 mmol) and 200 mg (0.136 mmol), the product yield increased from 84% to 96%. (**Table 1, entries 4 to 7**) This study reveals that increasing the quantity by a factor of five had no discernible effect on the product yield or reaction time. Therefore, 50 mg of **5** is sufficient to accelerate this model reaction and rapidly produce the required product.

**Table 1:** Catalyst loading optimization in synthesis of *N*-aryl sulfonamides



Entry	Catalyst	Quantity (mg)	Time (min.)	Yield <sup>b</sup> (%)
1.	bare $\text{Fe}_3\text{O}_4$ MNPs( <b>1</b> )	200	1440	-
2.	silica coated $\text{Fe}_3\text{O}_4$ MNPs ( <b>2</b> )	200	1440	-
3.	$\text{Fe}_3\text{O}_4@\text{silica-Lys}$ ( <b>4</b> )	200	1440	-
4.	$[\text{Fe}_3\text{O}_4@\text{silica-Lys-Cu}(\text{PPh}_3)\text{I}]$ complex ( <b>5</b> )	50	30	94
5.	$[\text{Fe}_3\text{O}_4@\text{silica-Lys-Cu}(\text{PPh}_3)\text{I}]$ complex ( <b>5</b> )	100	28	94
6.	$[\text{Fe}_3\text{O}_4@\text{silica-Lys-Cu}(\text{PPh}_3)\text{I}]$ complex ( <b>5</b> )	150	28	95
7.	$[\text{Fe}_3\text{O}_4@\text{silica-Lys-Cu}(\text{PPh}_3)\text{I}]$ complex ( <b>5</b> )	200	25	96

Reaction condition: phenyl boronic acid with (1.2 mmol), 4-toluenesulfonyl azide with (1.0 mmol), and ethanol with a volume of (5.0 mL); During chromatography, the yields that were isolated.

The selection of a solvent was the following phase in the process of optimization that was being carried out. To determine which of the many different solvents would be the most effective, a battery of rigorous tests was carried out on all of them (**Table 2**). **Table 2** illustrates that while enhances productivity has been procured in polar organic solvents such as dimethyl formamide (DMF), tetrahydrofuran (THF) and polar dichloromethane (DCM) (**entries 1-3**), only modest yields were achieved in non-polar solvents such as toluene and xylene. This is because polar organic solvents are more electronegative than non-polar solvents (**entries 4-7**). (**Table 2, entries 4-5**). In polar organic solvents like ethanol and methanol, adequate yields were found

(Table 2, entries 6-7). The fact that the reaction did not begin in the water came as a complete surprise to us (Table 2, entry 8). Ethanol produced the highest yield of the required product when compared to the other solvents that were investigated; hence, this solvent was chosen for more research. (Seen in Table 1, Position 7)

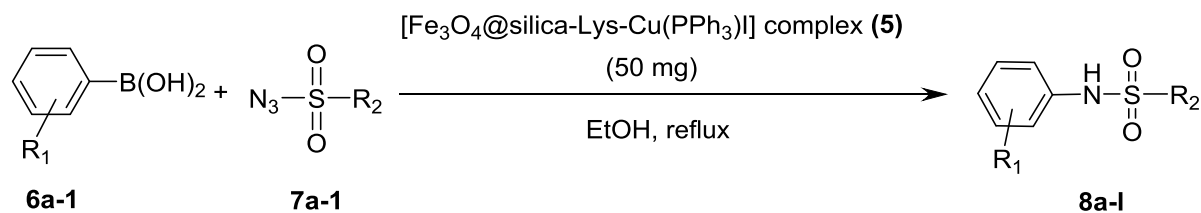
**Table 2:** Improvement of catalyst loading and solvent in N-aryl sulfamides synthesis

Entry	Solvent	Time (min)	Yield <sup>b</sup> (%)
1	DCM	420	74
2	DMF	480	72
3	THF	270	84
4	Toluene	540	62
5	Xylene	510	64
6	Methanol	50	84
<b>7</b>	<b>Ethanol</b>	<b>30</b>	<b>94</b>
8	Water	2881	Null Product

Reaction condition: phenyl boronic acid with (1.2 mmol), 4-toluenesulfonyl azide with (1.0 mmol) and ethanol with a volume of (5.0 mL); During chromatography, the yields that were isolated.

After figuring out the best conditions for the synthesis, the technique's applicability and versatility were tested by combining sulfonyl azides with various arylboronic acids in terms of their structural composition (Table 3). In every instance, the procedure was carried out as planned and resulted in the formation of the required N-aryl sulfonamides with yields ranging from high to exceptional (Table 3, entries 8 a-l) without any formation of any unintended byproducts. There was no impact from the electronic effect of substituents since the interactions between electron-rich and electron-poor arylboronic acids were equally successful in producing large yields of the compounds that were wanted.

**Table 3:**  $[\text{Fe}_3\text{O}_4@\text{silica-Lys-Cu}(\text{PPh}_3)\text{I}]$  complex (5) catalyzed N-aryl sulfonamides synthesis



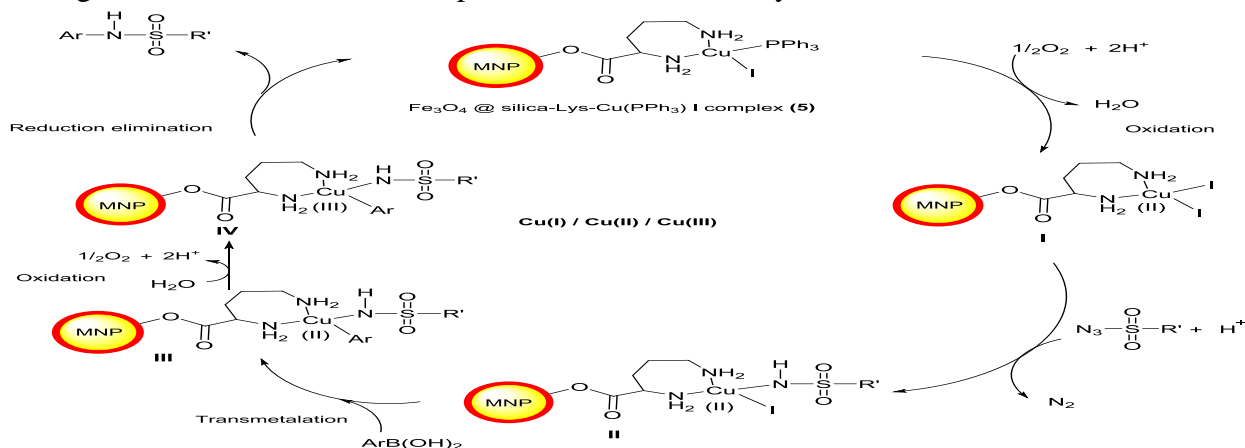
Entry	Phenyl boronic Acids (6)	Sulfonyl azides (7)	Product (8)	Time (Min.)	Yield <sup>b</sup> (%)
a				30	94
b				40	92
c				40	90
d				40	78
e				35	80
f				45	90
g				50	88
h				40	94
i				35	90
j				40	94

k				40	90
l				40	78

<sup>a</sup>Reaction conditions: : phenyl boronic acid with a concentration of 1.2 mmol, 4-toluenesulfonyl azide with a concentration of 1.0 mmol, and ethanol with a volume of 5.0 mL; [GrFemImi]NHC@Cu complex with a concentration of 100 mg; <sup>b</sup>extracted yields from chromatography.

The high catalytic activity of the [Fe<sub>3</sub>O<sub>4</sub>@silica-Lys-Cu(PPh<sub>3</sub>)I]complex (**5**) can be attributed to the presence of copper iodide and triphenylphosphine in the Chan-Lam coupling. Since triphenylphosphine is both an efficient reducing agent and a neutral ligand, it has found extensive use in the production of organometallic compounds. Copper combines with triphenylphosphine, which is reoxidized by atmospheric oxygen to facilitate reductive elimination, a crucial step in the coupling reaction. Consequently, the [Fe<sub>3</sub>O<sub>4</sub>@silica-Lys-Cu(PPh<sub>3</sub>)I]complex (**5**) accelerates the rate of reductive elimination, resulting in outstanding outcomes.

According to the Cu(I), Cu(II), and Cu(III) systems, the most likely mechanism of the [Fe<sub>3</sub>O<sub>4</sub>@silica-Lys-Cu(PPh<sub>3</sub>)I]complex (**5**) that catalyzed the Chan-Lam coupling is as follows: The research conducted by Kim and colleagues provides the foundation for [37], which is outlined in Scheme 3.7 is initially exposed to air and oxidised to form (I), which then reacts with sulfonyl azide to form an intermediate (II). In addition, intermediates result from the reaction of arylboronic acid with II, which is followed by transmetalation (III). Compound III is oxidised by air to produce an intermediate with a higher oxidation state (IV). This intermediate then undergoes reductive elimination to produce the desired *N*-aryl sulfonamides. [38]



**Scheme 3:** A possible framework for the formation of *N*-aryl sulfonamide using [Fe<sub>3</sub>O<sub>4</sub>@silica-Lys-Cu(PPh<sub>3</sub>)I]complex (**5**)

A split reaction test was conducted to determine the heterogeneity of the  $[\text{Fe}_3\text{O}_4@\text{silica-Lys-Cu}(\text{PPh}_3)\text{I}]$  complex (**5**). After 50% conversion, the **5** was removed from the reaction with the use of an external magnet (GC). The resulting filtrate was stirred for 6 hours under identical reaction conditions, and GC-MS analysis indicated no additional product production increase. Also, the ICP-OES measurement of the reaction mixture showed that there was no copper leaching, which suggests that the reactions are happening in different ways.

Reusability is an important characteristic of heterogeneous catalysts that determines their dynamic lifetime. In order to conduct experiments on reusability, the model reaction was conducted at optimal reaction conditions. The  $[\text{Fe}_3\text{O}_4@\text{silica-Lys-Cu}(\text{PPh}_3)\text{I}]$  complex (**5**) was easily retrieved after each cycle using an exterior magnet. The retrieved complex was once rinsed using ethanol and then dried in a vacuum at a temperature of  $50^\circ\text{C}$  before being reused in the subsequent cycle. The catalyst exhibited considerable reusability, with yields beginning at 94% and declining to 82% by the eighth run (**Fig. 8**). The fact that the recoverable complex can be used eight times without a big drop in output is clear.

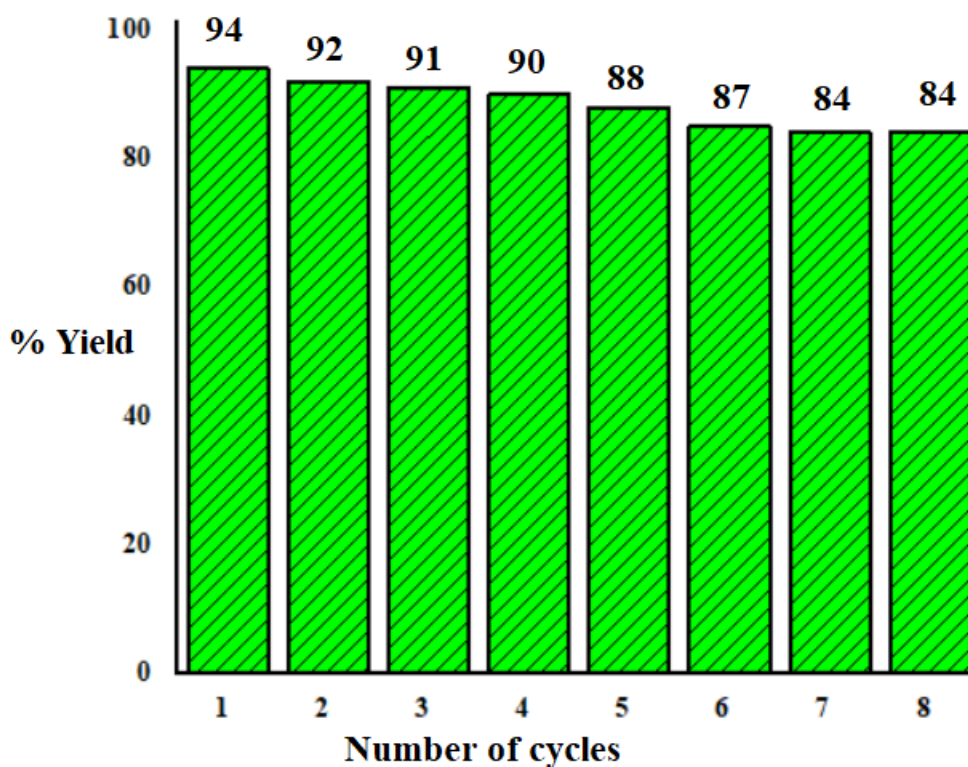


**Figure 8:** Reusability analysis of  $[\text{Fe}_3\text{O}_4@\text{silica-Lys-Cu}(\text{PPh}_3)\text{I}]$  complex (**5**) in N-aryl sulfonamide synthesis

In order to study the stability of the  $[\text{Fe}_3\text{O}_4@\text{silica-Lys-Cu}(\text{PPh}_3)\text{I}]$  complex, several technical studies, such as FT-Raman, TGA, FT-IR, TEM, and EDX, were conducted out on two fresh and recycled samples of the complex (**5**). It is important to note that the FT-IR spectra (**Fig. 9a**) of recovered **5** complex maintains the characteristic peak pattern of the fresh **5** complex (**Fig. 1d**). Figure 9b shows that the thermal analysis for recovered **5** in the TGA is quite similar to the thermogram for fresh **5**. (**Fig. 2b**). Following eight rounds of catalysis, the integrity of the catalyst was verified by elemental EDX mapping of the number **5**. (**Fig. 9c**). In more recent research, transmission electron microscopy (TEM) analysis of fresh (**Fig. 5 a-c**) and reused (**Fig. 9d**) **5** indicates that morphology is maintained even after six successive runs. After eight separate runs, the FT-Raman, TGA, FT-IR, TEM and EDX, examinations of fresh and recycled **5** demonstrated that the structural strength and key characteristics of the complex continue unaltered. This confirmed the stability of **5**.

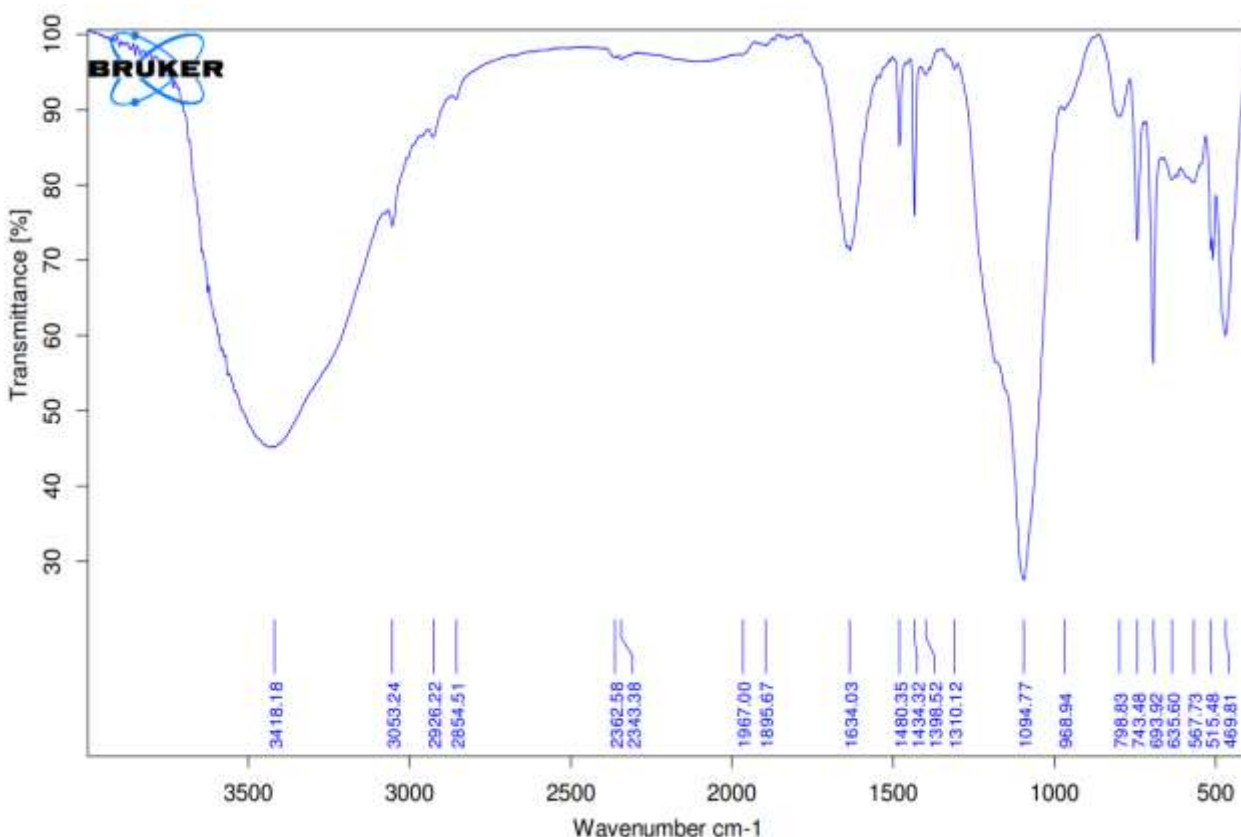


**Figure 9 (a):** FT-IR spectrum of reused  $[\text{Fe}_3\text{O}_4@\text{silica-Lys-Cu}(\text{PPh}_3)\text{I}]$  complex (**5**)

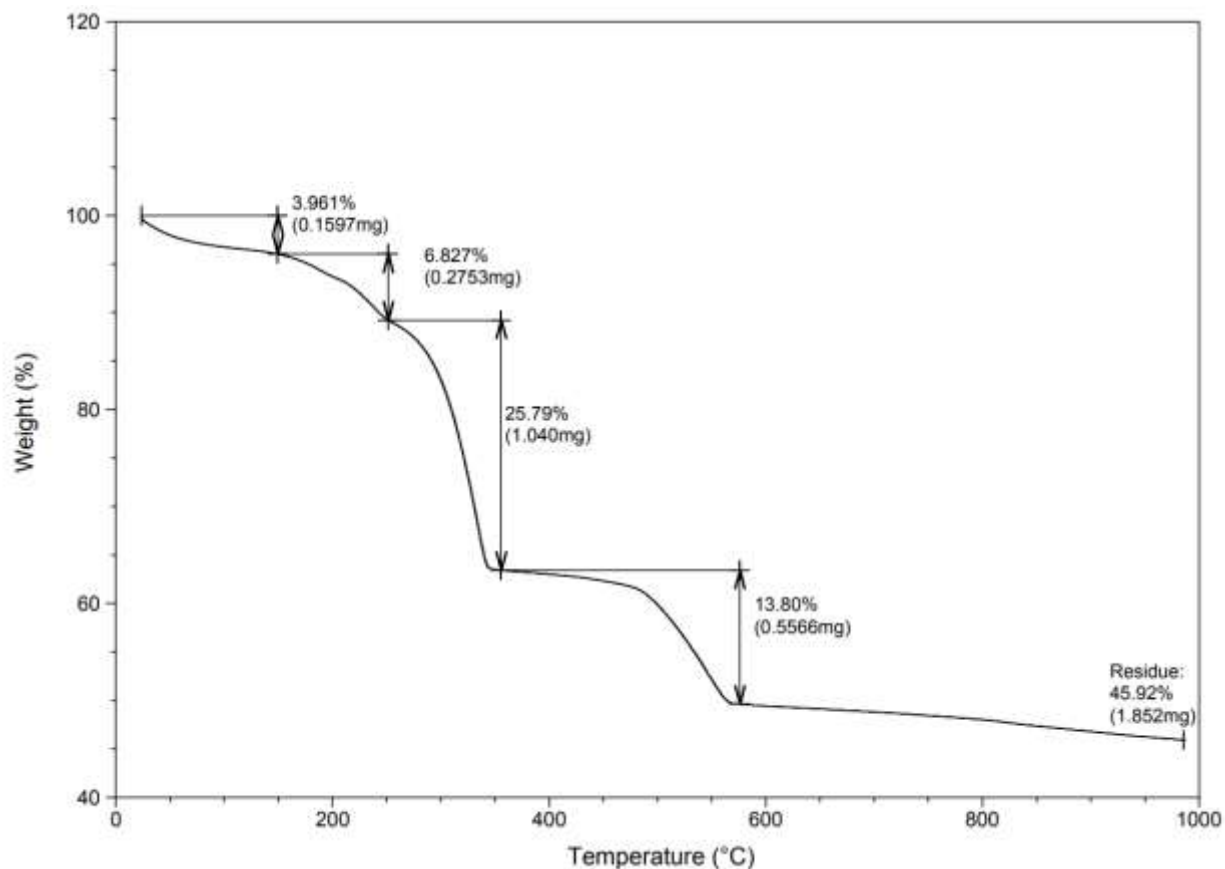


Figure 9 (b): TGA curve for recovered  $[\text{Fe}_3\text{O}_4@\text{silica-Lys-Cu}(\text{PPh}_3)\text{I}]$  complex (5)

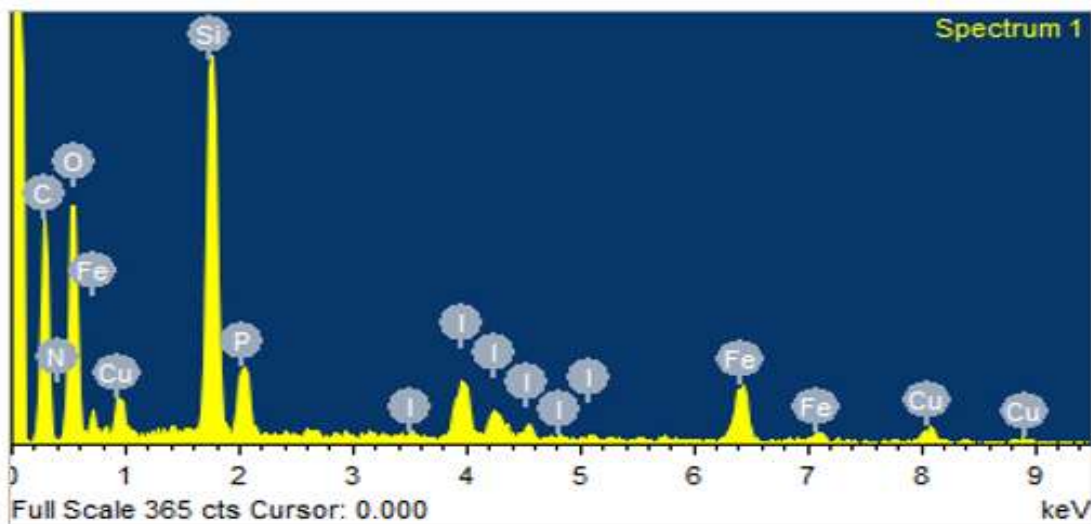
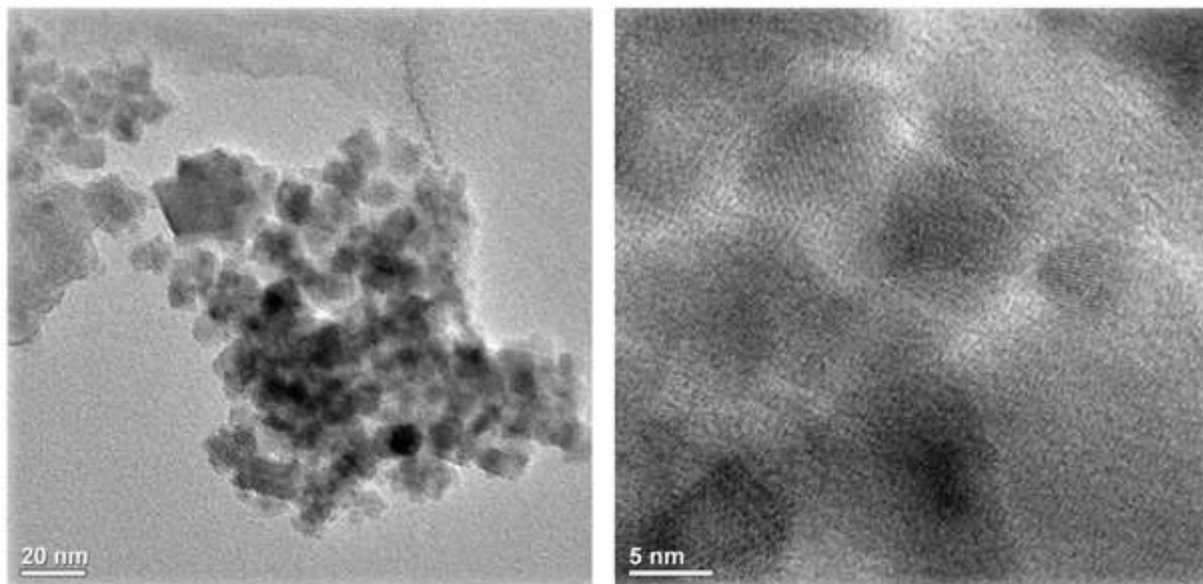


Figure 9 (C): EDX spectrum of reused  $[\text{Fe}_3\text{O}_4@\text{silica-Lys-Cu}(\text{PPh}_3)\text{I}]$  complex (5)



**Figure 9 (d):** TEM images of reused  $[\text{Fe}_3\text{O}_4@\text{silica-Lys-Cu}(\text{PPh}_3)\text{I}]$  complex (5)

#### **4. Conclusions**

In conclusion, we have described a newly established method for the environmentally friendly synthesis of N-aryl sulfonamides using magnetic nanoparticles containing copper as a reusable catalyst. Our team developed this methodology. XRD and TEM analysis revealed the crystalline  $\text{Fe}_3\text{O}_4$  MNPs single-phase inverse spinel structure, as well as their morphology and average diameter of 16 nm. In the Chan-Lam coupling of phenylboronic acids with sulfonyl azides, which results in the formation of N-aryl sulfonamides, the product of the reaction demonstrates excellent catalytic performance. This is the outcome of the reaction that was executed. This method provides a number of significant benefits, including high yields, a simple work-up process, the use of an environmentally friendly solvent, and a slightly shorter reaction time. These are additional benefits offered by this method:

#### **CONFLICT OF INTEREST**

The authors declare no conflict of interest

#### **Acknowledgements**

We gratefully acknowledge Indian Institute of Sciences (IISc), Bangalore and Sophisticated Analytical Instrumental Facility, Indian Institute of Technology, Bombay (IITB), Indian Institute of Technology, Madras (IITM), Northern East Hill University, Shillong (NEHU), Central Facility Center (CFC) Shivaji University, Kolhapur for providing spectral facilities.

## References

- [1] A. Dhakshinamoorthy, A. M. Asiri, H. Garcia (2015) Metal–organic frameworks catalyzed C–C and C–heteroatom coupling reactions. *Chem. Soc. Rev.* 44:1922-1947. <https://doi.org/10.1039/C4CS00254G>
- [2] a) J. Bariwal, E. Van der Eycken (2013) C–N bond forming cross-coupling reactions: an overview. *Chem. Soc. Rev.* 42:9283-9303. <https://doi.org/10.1039/C3CS60228A> b) S. H. Cho, J. Y. Kim, J. Kwak, S. Chang (2011) Recent advances in the transition metal-catalyzed twofold oxidative C–H bond activation strategy for C–C and C–N bond formation. *Chem. Soc. Rev.* 40:5068-5083. <https://doi.org/10.1039/C1CS15082K>
- [3] a) C. Sambigo, S. P. Marsden, A. J. Blacker, P. C. McGowan (2014) Copper catalysed Ullmann type chemistry: from mechanistic aspects to modern development. *Chem. Soc. Rev.* 43:3525-3550. <https://doi.org/10.1039/C3CS60289C> b) D. S. Surry, S. L. Buchwald (2011) Dialkylbiaryl phosphines in Pd-catalyzed amination: a user's guide. *Chem. Sci.* 2:27-50. <https://doi.org/10.1039/C0SC00331J> c) J. F. Hartwig (2008) Evolution of a Fourth Generation Catalyst for the Amination and Thioetherification of Aryl Halides. *Acc. Chem. Res.*, 41:1534-1544. <https://doi.org/10.1021/ar800098p>
- [4] (a) D. M. T. Chan, K. L. Monaco, R.-P. Wang, M. P. Winters (1998) New N- and O-arylations with phenylboronic acids and cupric acetate. *Tetrahedron Lett.* 39:2933-2936. [https://doi.org/10.1016/S0040-4039\(98\)00503-6](https://doi.org/10.1016/S0040-4039(98)00503-6) (b) P. Y. S. Lam, C. G. Clark, S. Saubern, J. Adams, M. P. Winters, D. M. T. Chan and A. Combs (1998) New aryl/heteroaryl C–N bond cross-coupling reactions via arylboronic acid/cupric acetate arylation. *Tetrahedron Lett.* 39:2941-2944. [https://doi.org/10.1016/S0040-4039\(98\)00504-8](https://doi.org/10.1016/S0040-4039(98)00504-8) (c) L. Naya, M. Larrosa, R. Rodriguez, J. Cruces (2012) Selective copper-promoted cross-coupling reaction of anilines and alkylboranes. *Tetrahedron Lett.* 53:769-772. <https://doi.org/10.1016/j.tetlet.2011.11.144>
- [5] I. Munir, A. F. Zahoor, N. Rasool, S. A. R. Naqvi, K. M. Zia, R. Ahmad (2019) Synthetic applications and methodology development of Chan–Lam coupling: a review. *Mol. Divers.* 23:215-259. <https://doi.org/10.1007/s11030-018-9870-z>
- [6] (a) Z. C. Zhang, B. Xu, X. Wang (2014) Engineering nanointerfaces for nanocatalysis. *Chem. Soc. Rev.* 43:7870-7886. <https://doi.org/10.1039/C3CS60389J> (b) I. I. Slowing, J. L. Vivero-Escoto, B. G. Trewyn, V. S. -Y. Lin (2010) Mesoporous silicananoparticles: structural design and applications. *J. Mater. Chem.* 20:7924-7937. <https://doi.org/10.1039/C0JM00554A> (c) P. Das, N. Aggarwal, N. R. Guha (2013) Solid supported Ru(0) nanoparticles: an efficient ligand-free heterogeneous catalyst for aerobic oxidation of benzylic and allylic alcohol to carbonyl. *Tetrahedron Lett.* 54:2924-2928. <https://doi.org/10.1016/j.tetlet.2013.03.106> (d) A. Corma, H. Garcia (2008) Supported gold nanoparticles as catalysts for organic reactions. *Chem. Soc. Rev.* 37:2096-2126. <https://doi.org/10.1039/B707314N> (e) C. J. Jia, F. Schuth (2011)

- Colloidal metal nanoparticles as a component of designed catalyst. *Phys. Chem. Chem. Phys.* 13:2457-2487. <https://doi.org/10.1039/C0CP02680H> (f) V. Polshettiwar, R. S. Varma (2010) Green chemistry by nano-catalysis. *Green Chem.* 12:743-754. <https://doi.org/10.1039/B921171C> (g) Q. M. Kainz, O. Reiser (2014) Polymer- and Dendrimer-Coated Magnetic Nanoparticles as Versatile Supports for Catalysts, Scavengers, and Reagents. *Acc. Chem. Res.* 47:667-677. <https://doi.org/10.1021/ar400236y> (h) R. K. Sharma, S. Sharma, S. Dutta, R. Zboril, M. B. Gawande (2015) Silica-nanosphere-based organic-inorganic hybrid nanomaterials: synthesis, functionalization and applications in catalysis. *Green Chem.* 17:3207-3230. <https://doi.org/10.1039/C5GC00381D> (i) R. K. Sharma, S. Sharma, G. Gaba, S. Dutta (2016) Coordinated copper(II) supported on silica nanospheres applied to the synthesis of  $\alpha$ -ketoamides via oxidative amidation of methyl ketones. *J. Mater. Sci.* 51:2121-2133. <https://doi.org/10.1007/s10853-015-9522-y> (j) R. K. Sharma, S. Sharma (2014) Silica nanosphere-supported palladium(ii) furfural complex as a highly efficient and recyclable catalyst for oxidative amination of aldehydes. *Dalton Trans.* 43:1292-1304. <https://doi.org/10.1039/C3DT51928G> (k) V. Polshettiwar, R. Luque, A. Fihri, H. Zhu, M. Bouhrara, J. -M. Basset (2011) Magnetically Recoverable Nanocatalysts. *Chem. Rev.* 111:3036-3075. <https://doi.org/10.1021/cr100230z> (l) F.-P. Ma, P. -H. Li, B. -L. Li, L. -P. Mo, N. Liu, H. -J. Kang, Y. -N. Liu, Z. -H. Zhang (2013) A recyclable magnetic nanoparticles supported antimony catalyst for the synthesis of N-substituted pyrroles in water. *Appl. Catal. A.* 457:34-41. <https://doi.org/10.1016/j.apcata.2013.03.005> (m) P. -H. Li, B. -L. Li, H. -C. Hu, X. -N. Zhao, Z. -H. Zhang (2014) Ionic liquid supported on magnetic nanoparticles as highly efficient and recyclable catalyst for the synthesis of  $\beta$ -keto enol ethers. *Catal. Commun.* 46:118-122. <https://doi.org/10.1016/j.catcom.2013.11.025> (n) S. Shylesh, V. Schünemann, W. R. Thiel (2010) Magnetically Separable Nanocatalysts: Bridges between Homogeneous and Heterogeneous Catalysis. *Angew. Chem. Int. Ed. Engl.* 49:3428-3459. <https://doi.org/10.1002/anie.200905684>
- [7] (a) M. Dabiri, N. F. Lehi, S. K. Movahed (2016) Fe<sub>3</sub>O<sub>4</sub>@RGO@Au@C Composite with Magnetic Core and Au Enwrapped in Double-Shelled Carbon: An Excellent Catalyst in the Reduction of Nitroarenes and Suzuki-Miyaura Cross-Coupling. *Catal. Lett.* 146:1674-1686. <https://doi.org/10.1007/s10562-016-1792-8> (b) A. Z. Wilczewska, I. Misztalewska (2014) Direct Synthesis of Imidazolium Salt on Magnetic Nanoparticles and Its Palladium Complex Application in the Heck Reaction. *Organometallics.* 33:5203-5208. <https://doi.org/10.1021/om500507q> (c) Y. Zhu, L. P. Stubbs, F. Ho, R. Liu, C. P. Ship, J. A. Maguire, N. S. Hosmane (2010) Magnetic Nanocomposites: A New Perspective in Catalysis. *ChemCatChem.* 2:365-374. <https://doi.org/10.1002/cctc.200900314> (d) M. Hajjami, S. Kolivand (2016) New metal complexes supported on Fe<sub>3</sub>O<sub>4</sub> magnetic nanoparticles as recoverable catalysts for selective oxidation of sulfides to sulfoxides. *Appl. Organometal. Chem.* 30(5):282-288.

- <https://doi.org/10.1002/aoc.3429> (e) L. Shiri, S. Zarei, M. Kazemi, D. Sheikh (2017) Sulfuric acid heterogenized on magnetic Fe<sub>3</sub>O<sub>4</sub> nanoparticles: A new and efficient magnetically reusable catalyst for condensation reactions. *Appl. Organometal. Chem.* 32(1):e3938. <https://doi.org/10.1002/aoc.3938> (f) H. Veisi, P. Mohammadi, J. Gholami (2014) Sulfamic acid heterogenized on functionalized magnetic Fe<sub>3</sub>O<sub>4</sub> nanoparticles with diaminoglyoxime as a green, efficient and reusable catalyst for one-pot synthesis of substituted pyrroles in aqueous phase. *Appl. Organometal. Chem.* 28(12):868-873. <https://doi.org/10.1002/aoc.3228> (g) J. Safaei-Ghomi, S. Zahedi (2015) L-Proline-functionalized Fe<sub>3</sub>O<sub>4</sub> nanoparticles as a novel magnetic chiral catalyst for the direct asymmetric Mannich reaction. *Appl. Organometal. Chem.* 29(8):566-571. <https://doi.org/10.1002/aoc.3333> (h) D. Azarifar, S. Mahmoudi-Gomyek, M. Ghaemi (2018) Immobilized Cu(II) Schiff base complex supported on Fe<sub>3</sub>O<sub>4</sub> magnetic nanoparticles: A highly efficient and reusable new catalyst for the synthesis of pyranopyridine derivatives. *Appl. Organometal. Chem.* 32(12):e4541. <https://doi.org/10.1002/aoc.4541> (i) F. Kamali, F. Shirini (2018) Fe<sub>3</sub>O<sub>4</sub>@SiO<sub>2</sub>-ZrCl<sub>2</sub>-MNPs: A novel magnetic catalyst for the clean and efficient cascade synthesis of 1-(benzothiazolylamino)methyl-2-naphthol derivatives in the absence of solvent. *Appl. Organometal. Chem.* 32(1):e3972. <https://doi.org/10.1002/aoc.3972> (j) D. Habibi, S. Heydari, M. Afsharfarnia, F. Moghimpour (2018) Preparation of novel palladium nanoparticles supported on magnetic iron oxide and their catalytic application in the synthesis of 2-imino-3-phenyl-2,3-dihydrobenzo[d]oxazol-5-ols. *Appl. Organometal. Chem.* 32(4):e4263. <https://doi.org/10.1002/aoc.4263> (k) K. Manjunatha, T. S. Koley, V. Kandathil, R. B. Dateer, G. Balakrishna, B. S. Sasidhar, S. A. Patil, S. A. Patil (2018) Magnetic nanoparticle-tethered Schiff base-palladium(II): Highly active and reusable heterogeneous catalyst for Suzuki-Miyaura cross-coupling and reduction of nitroarenes in aqueous medium at room temperature. *Appl. Organometal. Chem.* 32(4):e4266. <https://doi.org/10.1002/aoc.4266> (l) S. Rostamnia, B. Gholipour, X. Liu, Y. Wang, H. Arandiyan (2018) NH<sub>2</sub>-coordinately immobilized tris(8-quinolinolato)iron onto the silica coated magnetite nanoparticle: Fe<sub>3</sub>O<sub>4</sub>@SiO<sub>2</sub>-FeQ<sub>3</sub> as a selective Fenton-like catalyst for clean oxidation of sulfides. *J. Colloid Interface Sci.* 511:447-455. <https://doi.org/10.1016/j.jcis.2017.10.028> (m) E. Doustkhah, M. Heidarizadeh, S. Rostamnia, A. Hassankhani, B. Kazemi, X. Liu (2018) Copper immobilization on carboxylic acid-rich Fe<sub>3</sub>O<sub>4</sub>-Pectin: Cu<sup>2+</sup>@Fe<sub>3</sub>O<sub>4</sub>-Pectin a superparamagnetic nanobiopolymer source for click reaction. *Mater. Lett.* 216:139-143. <https://doi.org/10.1016/j.matlet.2018.01.014> (n) E. Doustkhah, S. Rostamnia, B. Gholipour, B. Zeynizadeh, A. Baghban, R. Luque (2017) Design of chitosan-dithiocarbamate magnetically separable catalytic nanocomposites for greener aqueous oxidations at room temperature. *Mol. Catal.* 434:7-15. <https://doi.org/10.1016/j.mcat.2017.01.031> (o) S. Rostamnia, B. Zeynizadeh, E.

- Doustkhah, A. Baghban, K. O. Aghbash (2015) The use of  $\kappa$ -carrageenan/Fe<sub>3</sub>O<sub>4</sub> nanocomposite as a nanomagnetic catalyst for clean synthesis of rhodanines. *Catal. Commun.* 68:77-83. <https://doi.org/10.1016/j.catcom.2015.05.002>
- [8] (a) P. B. Shete, R. M. Patil, N. D. Thorat, A. Prasad, R. S. Ningthoujam, S. J. Ghosh, S. H. Pawar (2014) Magnetic chitosan nanocomposite for hyperthermia therapy application: Preparation, characterization and in vitro experiments. *Appl. Surf. Sci.* 288:149-157. <https://doi.org/10.1016/j.apsusc.2013.09.169> (b) J. Devkota, T. T. T. Mai, K. Stojak, P. T. Ha, H. N. Pham, X. P. Nguyen, P. Mukherjee, H. Srikanth, M. H. Phan (2014) Synthesis, inductive heating, and magnetoimpedance-based detection of multifunctional Fe<sub>3</sub>O<sub>4</sub> nanoconjugates. *Sens. Actuators B Chem.* 190:715-722. <https://doi.org/10.1016/j.snb.2013.09.033> (c) P. B. Shete, R. M. Patil, B. M. Tiwale, S. H. Pawar (2015) Water dispersible oleic acid-coated Fe<sub>3</sub>O<sub>4</sub> nanoparticles for biomedical applications. *J. Magn. Mater.* 377:406-410 <https://doi.org/10.1016/j.jmmm.2014.10.137> (d) S. Kumari, R. P. Singh (2012) Glycolic acid-g-chitosan-Pt-Fe<sub>3</sub>O<sub>4</sub> nanoparticles nanohybrid scaffold for tissue engineering and drug delivery. *Int. J. Biol. Macromol.* 51:76-82. <https://doi.org/10.1016/j.ijbiomac.2012.01.040> (e) H. Hashemi-Moghaddam, S. Kazemi-Bagsangani, M. Jamili, S. Zavareh (2016) Evaluation of magnetic nanoparticles coated by 5-fluorouracil imprinted polymer for controlled drug delivery in mouse breast cancer model. *Int. J. Pharm.* 497(1-2):228-238. <https://doi.org/10.1016/j.ijpharm.2015.11.040> (f) H. Jiang, D. Jiang, J. Shao, X. Sun (2016) Magnetic molecularly imprinted polymer nanoparticles based electrochemical sensor for the measurement of Gram-negative bacterial quorum signaling molecules (N-acyl-homoserine-lactones). *Biosens. Bioelectron.* 75:411-419. <https://doi.org/10.1016/j.bios.2015.07.045>
- [9] (a) X. Liu, X. Lu, Y. Huang, C. Liu, S. Zhao (2014) Fe<sub>3</sub>O<sub>4</sub>@ionic liquid@methyl orange nanoparticles as a novel nano-adsorbent for magnetic solid-phase extraction of polycyclic aromatic hydrocarbons in environmental water samples. *Talanta.* 119:341-347. <https://doi.org/10.1016/j.talanta.2013.11.039> (b) J. Mao, W. Jiang, J. Gu, S. Zhou, Y. Lu, T. Xie (2014) Synthesis of P (St-DVB)/Fe<sub>3</sub>O<sub>4</sub> microspheres and application for oil removal in aqueous environment. *Appl. Surf. Sci.* 317:787-793. <https://doi.org/10.1016/j.apsusc.2014.08.191> (c) J. Xu, J. Tang, S. A. Baig, X. Lv, X. Xu (2013) Enhanced dechlorination of 2,4-dichlorophenol by Pd/Fe single bond Fe<sub>3</sub>O<sub>4</sub> nanocomposites. *J. Hazard. Mater.* 244-245:628-636. <https://doi.org/10.1016/j.jhazmat.2012.10.051>
- [10] (a) Y. R. Cui, C. Hong, Y. L. Zhou, Y. Li, X. M. Gao, X. X. Zhang (2011) Synthesis of orientedly bioconjugated core/shell Fe<sub>3</sub>O<sub>4</sub>@Au magnetic nanoparticles for cell separation. *Talanta* 85:1246-1252. <https://doi.org/10.1016/j.talanta.2011.05.010> (b) L.

- Chen, C. Guo, Y. Guan, H. Liu (2007) Isolation of lactoferrin from acid whey by magnetic affinity separation. *Sep. Sci. Technol.* 56:168-174. <https://doi.org/10.1016/j.seppur.2007.01.019> (c) Z. -Y. Ma, X. -Q. Liu, Y. -P. Guan, H. -Z. Liu (2006) Synthesis of magnetic silica nanospheres with metal ligands and application in affinity separation of proteins. *Colloids Surf. A Physicochem. Eng. Asp.* 275:87-91. <https://doi.org/10.1016/j.colsurfa.2005.04.045>
- [11] (a) S. Laurent, D. Forge, M. Port, A. Roch, C. Robic, L. Vander Elst, R. N. Muller (2008) Magnetic Iron Oxide Nanoparticles: Synthesis, Stabilization, Vectorization, Physicochemical Characterizations, and Biological Applications. *Chem. Rev.* 108:2064-2110. <https://doi.org/10.1021/cr068445e> (b) H. -P. Peng, R. -P. Liang, J. D. Qiu (2011) Facile synthesis of Fe<sub>3</sub>O<sub>4</sub>@Al<sub>2</sub>O<sub>3</sub> core-shell nanoparticles and their application to the highly specific capture of heme proteins for direct electrochemistry. *Biosens. Bioelectron.* 26:3005-3011. <https://doi.org/10.1016/j.bios.2010.12.003> (c) J. Wu, L. Zhou, H. Zhang, J. Guo, X. Mei, C. Zhang, J. Yuan, X. -H. Xing (2014) Direct affinity immobilization of recombinant heparinase I fused to maltose binding protein on maltose-coated magnetic nanoparticles. *Biochem. Eng. J.* 90:170-177. <https://doi.org/10.1016/j.bej.2014.05.021>
- [12] (a) M. H. Mashhadizadeh, M. Amoli-Diva, M. R. Shapouri, H. Afruzi (2014) Solid phase extraction of trace amounts of silver, cadmium, copper, mercury, and lead in various food samples based on ethylene glycol bis-mercaptoacetate modified 3-(trimethoxysilyl)-1-propanethiol coated Fe<sub>3</sub>O<sub>4</sub> nanoparticles. *Food Chem.* 151:300-305. <https://doi.org/10.1016/j.foodchem.2013.11.082> (b) X. Liu, L. Zhang, J. Zeng, Y. Gao, Z. Tang (2013) Superparamagnetic nano-immunobeads toward food safety insurance. *J. Nanoparticle Res.* 15:1796. <https://doi.org/10.1007/s11051-013-1796-x>
- [13] (a) M. S. Abaee, E. Doustkhah, M. Mohammadi, M. M. Mojtahedi, K. Harms (2016) Tandem aldol condensation-Diels-Alder-aromatization sequence of reactions: a new pathway for the synthesis of 2-tetralone derivatives. *Can. J. Chem.* 94:733. <https://doi.org/10.1139/cjc-2016-0246> (b) E. Doustkhah, S. Rostamnia (2016) Covalently bonded sulfonic acid magnetic graphene oxide: Fe<sub>3</sub>O<sub>4</sub>@GO-Pr-SO<sub>3</sub>H as a powerful hybrid catalyst for synthesis of indazolophthalazinetriones. *J. Colloid Interface Sci.* 478:280-287. <https://doi.org/10.1016/j.jcis.2016.06.020> (c) G. Liu, J. Gao, H. Ai, X. Chen (2013) Applications and Potential Toxicity of Magnetic Iron Oxide Nanoparticles. *Small*, 9(9-10):1533. <https://doi.org/10.1002/sml.201201531>
- [14] (a) J. B. M. de Resende Filho, G. P. Pires, J. M. G. de Oliveira Ferreira, E. E. S. Teotonio, J. A. Vale, (2017) Knoevenagel Condensation of Aldehydes and Ketones with Malononitrile Catalyzed by Amine Compounds-Tethered Fe<sub>3</sub>O<sub>4</sub>@SiO<sub>2</sub> Nanoparticles. *Catal. Lett.*, 147:167-180. <https://doi.org/10.1007/s10562-016-1916-1> (b) M. B.

- Gawande, P. S. Branco, R. S. Varma (2013) Nano-magnetite ( $\text{Fe}_3\text{O}_4$ ) as a support for recyclable catalysts in the development of sustainable methodologies. *Chem. Soc. Rev.* 42:3371-3393. <https://doi.org/10.1039/C3CS35480F> (c) B. Karimi, F. Mansouri, H. M. Mirzaei (2015) Recent Applications of Magnetically Recoverable Nanocatalysts in C-C and C-X Coupling Reactions. *ChemCatChem.* 7:1736-1789. <https://doi.org/10.1002/cctc.201403057>
- [15] (a) J. Yuan, Y. Xu, A. H. E. Muller (2011) One-dimensional magnetic inorganic-organic hybrid nanomaterials. *Chem. Soc. Rev.* 40:640-655. <https://doi.org/10.1039/C0CS00087F> (b) M. Esmaeilpour, A. R. Sardarian, J. Javidi (2014) Synthesis and characterization of Schiff base complex of Pd(II) supported on superparamagnetic  $\text{Fe}_3\text{O}_4@SiO_2$  nanoparticles and its application as an efficient copper- and phosphine ligand-free recyclable catalyst for Sonogashira-Hagihara coupling reactions. *J. Organomet. Chem.* 749:233-240. <https://doi.org/10.1016/j.jorganchem.2013.10.011> (c) H. Keypour, S. G. Saremi, M. Noroozi, H. Veisi (2017) Synthesis of magnetically recyclable  $\text{Fe}_3\text{O}_4@[(\text{EtO})_3\text{Si-L1H}]/\text{Pd(II)}$  nanocatalyst and application in Suzuki and Heck coupling reactions. *Appl. Organometal. Chem.* 31:3558. <https://doi.org/10.1002/aoc.3558> (d) S. B. Lima, S. M. S. Borges, M. do Carmo Rangel, S. G. Marchetti (2013) Effect of iron content on the catalytic properties of activated carbon-supported magnetite derived from biomass. *J. Braz. Chem. Soc.* 24(2):344. <https://doi.org/10.5935/0103-5053.20130044>
- [16] a) W.G. Harter, H. Albrecht, K. Brady, B. Caprathe, J. Dunbar, J. Gilmore, S. Hays, C. R. Kostlan, B. Lunney, N. Walker (2004) The design and synthesis of sulfonamides as caspase-1 inhibitors. *Bioorg. Med. Chem. Lett.* 14:809-812. <https://doi.org/10.1016/j.bmcl.2003.10.065> b) S. Moon, J. Nam, Kris Rathwell, W. Kim (2014) Copper-Catalyzed Chan-Lam Coupling between Sulfonyl Azides and Boronic Acids at Room Temperature. *Org. Lett.* 16(2):338-341. <https://doi.org/10.1021/ol403717f> c) B.R. Stranix, J.F. Lavallee, G. Sevigny, J. Yelle, V. Perron, N. Leberre, D. Herbart, J.J. Wu (2006) Lysine sulfonamides as novel HIV-protease inhibitors: N $\epsilon$ -Acyl aromatic  $\alpha$ -amino acids. *Bioorg. Med. Chem. Lett.* 16:3459-3462. <https://doi.org/10.1016/j.bmcl.2006.04.011> d) A. Scozzafava, T. Owa, A. Mastrolorenzo, C.T. Supuran (2003) Anticancer and Antiviral Sulfonamides. *Curr. Med. Chem.* 10:925-953. <https://doi.org/10.2174/0929867033457647> e) C.T. Supuran, A. Casini, A. Scozzafava (2003) Protease inhibitors of the sulfonamide type: Anticancer, antiinflammatory, and antiviral agents. *Med. Res. Rev.* 23:535-558. <https://doi.org/10.1002/med.10047>
- [17] a) S.Y. Moon, J. Nam, K. Rathwell, W.S. Kim (2014) Copper-Catalyzed Chan-Lam Coupling between Sulfonyl Azides and Boronic Acids at Room Temperature. *Org. Lett.* 16:338-341. <https://doi.org/10.1021/ol403717f> b) D.M.T. Chan, K.L. Monaco, R.P. Wang, M.P. Winters (1998) New N- and O-arylations with phenylboronic acids and cupric acetate. *Tet. Lett.* 39:2933-2936. [https://doi.org/10.1016/S0040-4039\(98\)00503-6](https://doi.org/10.1016/S0040-4039(98)00503-6)

- [18] M. Khalaj, M. Ghazanfarpour-Darjani, M. Reza, T.B. Olyai, S.F. Shamami (2016) Palladium nanoparticles as reusable catalyst for the synthesis of N-aryl sulfonamides under mild reaction conditions. *J. Sulfur Chem.* 37:211-221. <https://doi.org/10.1080/17415993.2015.1122010>
- [19] B. Ouyang, D. Liu, K. Xia, Y. Zheng, H. Mei, G. Qiu (2018) Synthesis of N-Arylsulfonamides by a Copper-Catalyzed Reaction of Chloramine-T and Arylboronic Acids at Room Temperature. *Synlett.* 29:111-115. <http://dx.doi.org/10.1055/s-0036-1590978>
- [20] a) B.R. Rosen, J.C. Ruble, T.J. Beauchamp, A. Navarro (2011) Mild Pd-Catalyzed N-Arylation of Methanesulfonamide and Related Nucleophiles: Avoiding Potentially Genotoxic Reagents and Byproducts. *Org. Lett.* 13:2564-2567. <https://doi.org/10.1021/ol200660s> b) Z. Liu, R.C. Larock (2006) Facile N-Arylation of Amines and Sulfonamides and O-Arylation of Phenols and Arenecarboxylic Acids. *J. Org. Chem.* 71:3198-3209. <https://doi.org/10.1021/jo0602221> c) B. Nguyen, E.J. Emmett, M. C. Willis (2010) Palladium-Catalyzed Aminosulfonylation of Aryl Halides. *J. Am. Chem. Soc.* 132:16372-16373. <https://doi.org/10.1021/ja1081124> d) W. Zhang, J. Xie, B. Rao, M. Luo (2015) Iron-Catalyzed N-Arylsulfonamide Formation through Directly Using Nitroarenes as Nitrogen Sources. *J. Org. Chem.* 80:3504-3511. <https://doi.org/10.1021/acs.joc.5b00130>
- [21] (a) R. Kurane, J. Jadhav, S. Khanpure, R. Salunkhe, G. Rashinkar (2013) Synergistic catalysis by an aerogel supported ionic liquid phase (ASILP) in the synthesis of 1,5-benzodiazepines. *Green Chem.* 15:1849-1856. <https://doi.org/10.1039/C3GC40592C> (b) S. Gajare, M. Jagadale, A. Naikwade, P. Bansode, G. Rashinkar (2019) Facile Chan-Lam coupling using ferrocene tethered N-heterocyclic carbene-copper complex anchored on graphene. *Appl. Organomet. Chem.* 33:e4915. <https://doi.org/10.1002/aoc.4915> (c) S. Khanpure, M. Jagadale, D. Kale, S. Gajare, G. Rashinkar (2019) Cellulose-Supported Ionic Liquid Phase Catalyst-Mediated Mannich Reaction. *Aust. J. Chem.* 72:513-523. <https://doi.org/10.1071/CH18576> (d) S. Gajare, A. Patil, D. Kale, P. Bansode, P. Patil G. Rashinkar (2019) Graphene Oxide-Supported Ionic Liquid Phase Catalyzed Synthesis of 3,4-Dihydro-2H-naphtho[2,3-e][1,3]oxazine-5,10-diones. *Cat. Letters.* 150:243-255. <https://doi.org/10.1007/s10562-019-02934-0>
- [22] X. Zhao, Y. Shi, T. Wang, Y. Cai, G. Jiang (2008) Preparation of silica-magnetite nanoparticle mixed hemimicelle sorbents for extraction of several typical phenolic compounds from environmental water samples. *J. Chromatogr. A.* 1188:140-147. <https://doi.org/10.1016/j.chroma.2008.02.069>
- [23] Q. Liu, Z. Xu, J. A. Finch, R. Egerton (1998) A Novel Two-Step Silica-Coating Process for Engineering Magnetic Nanocomposites. *Chem. Mater.* 10:3936-3940. <https://doi.org/10.1021/cm980370a>

- [24] M. Kooti, M. Afshari (2012) Phosphotungstic acid supported on magnetic nanoparticles as an efficient reusable catalyst for epoxidation of alkenes. *Mater. Res. Bull.* 47:3473-3478. <https://doi.org/10.1016/j.materresbull.2012.07.001>
- [25] Y. Tamer, B. Chen (2018) Lysine-derived, pH-sensitive and biodegradable poly(beta-aminoester urethane) networks and their local drug delivery behavior. *Soft Matter.* 14:1195-1209. <https://doi.org/10.1039/C7SM01886J>
- [26] K. Azizi, M. Karimi, H. R. Shaterian, A. Heydari (2014) Ultrasound irradiation for the green synthesis of chromenes using l-arginine-functionalized magnetic nanoparticles as a recyclable organocatalyst. *RSC Adv.* 4:42220-42225. <https://doi.org/10.1039/C4RA06198E>
- [27] G. Costa, E. Reisenhofer, L. Stefani (1965) Complexes of copper (I) with triphenylphosphine. *J. Inorg. Nucl. Chem.* 27:2581-2584. [https://doi.org/10.1016/0022-1902\(65\)80159-2](https://doi.org/10.1016/0022-1902(65)80159-2)
- [28] T. S. Lobana, R. Sultana, G. Hundal (2008) Heterocyclic thioamides of copper(I): Synthesis and crystal structures of copper complexes with 1,3-imidazoline-2-thiones in the presence of triphenyl phosphine. *polyhedron.* 27:1008-1016. <https://doi.org/10.1016/j.poly.2007.11.036>
- [29] Y. Cui, D. Huang, Y. Li, W. Huang, Z. Liang, Z. Xua, S. Zhao (2015) Aluminium nanoparticles synthesized by a novel wet chemical method and used to enhance the performance of polymer solar cells by the plasmonic effect. *J. Mater. Chem. C.* 3:4099-4103. <https://doi.org/10.1039/C5TC00213C>
- [30] D. Hu, X. Wan, X. Li, J. Liu, C. Zhou (2017) Synthesis of water-dispersible poly-l-lysine-functionalized magnetic Fe<sub>3</sub>O<sub>4</sub>-(GO-MWCNTs) nanocomposite hybrid with a large surface area for high-efficiency removal of tartrazine and Pb(II). *Int. J. Biol. Macromol.* 105:1611-1621. <https://doi.org/10.1016/j.ijbiomac.2017.03.010>
- [31] A. M. Demin, A. V. Mekhaev, O. F. Kandarakov, V. I. Popenko, O. G Leonova, A. M. Murzakaev, D. K. Kuznetsov, M. A. Uimin, A. S. Minin, V. Y. Shur, A. V. Belyavsky, V. P. Krasnov (2020) L-Lysine-modified Fe<sub>3</sub>O<sub>4</sub> nanoparticles for magnetic cell labeling. *Colloids Surf. B.* 190:110879. <https://doi.org/10.1016/j.colsurfb.2020.110879>
- [32] Y. Hu, L. J. Meng, L. Niu, Q. H. Lu (2013) Highly Cross-Linked and Biocompatible Polyphosphazene-Coated Superparamagnetic Fe<sub>3</sub>O<sub>4</sub> Nanoparticles for Magnetic Resonance Imaging. *Langmuir.* 29:9156-9163. <https://doi.org/10.1021/la402119s>
- [33] M. Nasrollahzadeh, A. Ehsani, M. Maham (2014) Copper-Catalyzed N-Arylation of Sulfonamides with Boronic Acids in Water under Ligand-Free and Aerobic Conditions. *Synlett.* 25:505-508. <https://dx.doi.org/10.1055/s-0033-1340475>
- [34] S. Ghosh, A. Z. M. Badruddoza, M. S. Uddin, K. Hidajat (2011) Adsorption of chiral aromatic amino acids onto carboxymethyl-β-cyclodextrin bonded Fe<sub>3</sub>O<sub>4</sub>/SiO<sub>2</sub> core-shell nanoparticles. *J. Colloid Interface Sci.* 354:483-492. <https://doi.org/10.1016/j.jcis.2010.11.060>

- [35] A. Nia, S. Rana, D. Dçhler, F. Jirsa, A. Meister, L. Guadagno, E. Koslowski, M. Bron, W.H. Binder (2015) Carbon-Supported Copper Nanomaterials: Recyclable Catalysts for Huisgen [3+2] Cycloaddition Reactions. *Chem. Eur. J.* 21:10763. <https://doi.org/10.1002/chem.201501217>
- [36] L. Ji, L. Zhou, X. Bai, Y. Shao, G. Zhao, Y. Qu, C. Wanga, Y. Li (2012) Facile synthesis of multiwall carbon nanotubes/iron oxides for removal of tetrabromobisphenol A and Pb(ii). *J. Mater. Chem.* 22:15853. <https://doi.org/10.1039/C2JM32896H>
- [37] a) S. Moon, J. Nam, K. Rathwell, W. Kim (2014) Copper-Catalyzed Chan–Lam Coupling between Sulfonyl Azides and Boronic Acids at Room Temperature. *Org. Lett.* 16(2):338. <https://doi.org/10.1021/ol403717f> b) P.Y.S. Lam, G. Clark, S. Saubern, J. Adams, K.M. Averill, D.T.M. Chan, A. Combs (2000) Copper Promoted Aryl/Saturated Heterocyclic C-N Bond Cross-Coupling with Arylboronic Acid and Arylstannane. *Synlett.* (5):0674-0676. <https://doi.org/10.1039%2Fc8ra09219b>
- [38] A.E. King, L.M. Huffman, A. Casitas, M. Costas, X. Ribas, S.S. Stahl (2010) Copper-Catalyzed Aerobic Oxidative Functionalization of an Arene C–H Bond: Evidence for an Aryl-Copper(III) Intermediate. *J. Am. Chem. Soc.* 132(34):12068. <https://doi.org/10.1021/ja1045378>